

Centralized Fairness for Redistricting

Seyed A. Esmaili¹, Darshan Chakrabarti², Hayley Grape³, and Brian Brubach³

¹University of Maryland, College Park

²Columbia University

³Wellesley College

Abstract

In representative democracy, the electorate is often partitioned into districts with each district electing a representative. Unfortunately, these systems have proven vulnerable to the practice of partisan gerrymandering. As a result, methods for detecting gerrymandered maps were introduced and have led to significant success. However, the question of how to draw district maps in a principled manner remains open with most of the existing literature focusing on optimizing certain properties such as geographical compactness or partisan competitiveness. In this work, we take an alternative approach which seeks to find the most “typical” redistricting map. More precisely, we introduce a family of well-motivated distance measures over redistricting maps. Then, by generating a large collection of maps using sampling techniques, we select the map which minimizes the sum of the distances from the collection, i.e., the most “central” map. We produce scalable, linear-time algorithms and derive sample complexity guarantees. We show that a by-product of our approach is the ability to detect gerrymandered maps as they are found to be outlier maps in terms of distance.

1 Introduction

Redistricting is the process of dividing an electorate into a collection of districts which each elect a representative. In the United States, this process is used for both federal and state-level representation, and we will use the U.S. House of Representatives as a running example throughout this paper. Subject to both state and federal law, the division of states into congressional districts is not arbitrary and must satisfy a collection of properties such as districts being contiguous and of near-equal population. Despite these regulations, it is clear that redistricting is vulnerable to strategic manipulation in the form of gerrymandering. The body in charge of redistricting can easily create a map within the legal constraints that leads to election results which favor a particular outcome (e.g., more representatives elected from one political party in the case of *partisan gerrymandering*). In addition, the ability to draw gerrymandered districts has improved greatly with the aid of computers since the historic salamander-shaped district approved by Massachusetts Governor Elbridge Gerry in 1812. For example, assuming voting consistent with the 2016 election, the state of North Carolina with 13 representatives can be redistricted to elect either 3 Democrats and 10 republicans or 10 Democrats and 3 Republicans. This represents a potential 14 seat swing due to redistricting while at the time of this writing, the Democratic Party controls a majority of the 435 voting members of the House of Representatives with only 11 seats more than the opposing party.

However, despite this obvious threat to functioning democracy, partisan gerrymandering has often eluded regulation partly because it has been difficult to measure. In response, a recent line of

research introduced sampling techniques to randomly¹ generate a large collection of redistricting maps [Chikina et al., 2017, DeFord et al., 2019, Herschlag et al., 2020] and calculate statistics such as a histogram of the number of seats won by each party using this collection. With these statistics, one can check if a proposed or enacted map is an outlier with respect to the sample. For example, the 2012 redistricting map of North Carolina produced 4 seats for the democratic party whereas 95% of the sampled maps led to between 6 and 9 seats [Mattingly and Vaughn, 2014]. In fact, these techniques were used as a key argument in the most recent U.S. Supreme Court case on gerrymandering [Rucho v. Common Cause, 2019] and have supported successful efforts to change redistricting maps in state supreme court cases [LWV vs Commonwealth of Pennsylvania, 2018]. More importantly for the present work, at least two states, Michigan and Wisconsin, will use such a sampling tool [DeFord et al., 2019] in the current redistricting process in response to the 2020 U.S. Census [Chen, 2021].

While great progress has been made in recent years on the problem of detecting/labeling possible gerrymandering through the use of these sampling techniques which can quantify outlier characteristics in a given map, the question of drawing a redistricting map in a way that is “fair” and immune to strategic manipulation remains largely unclear. We survey some existing proposals to automate redistricting in more detail in Section 2, but none of them have been adopted in practice thus far. The direction most commonly proposed by automated redistricting methods is to cast redistricting as a constrained optimization problem [Cohen-Addad et al., 2018, Hettle et al., 2021, Liu et al., 2016], with objectives such as compactness and a collection of common constraints (district contiguity, equal population, etc.). However, formulating redistricting as an optimization problem poses an issue in the fact that there are multiple desired properties, and it is not clear why one should be optimized for over others.

Indeed, since there is collection of redistricting maps that can be considered valid or legal, it seems quite reasonable to attempt to output the most “typical” map. Inspired by social choice theory (in particular, the Kemeny rule [Kemeny, 1959, Brandt et al., 2016]), we propose a redistricting procedure in which the most typical (central) map among a given collection is selected. More precisely, we introduce a family of distance functions over redistricting maps and then select the map which minimizes the sum of distances to the other maps.

1.1 Our Contributions

We introduce the novel approach of choosing a *central* map among a set of redistricting maps and propose a method for identifying such a map. More concretely, we define a family of distances over redistricting maps and give algorithms that can find the medoid of a collection of given maps. Our family of distances is simple and interpretable and can accommodate various considerations such as the population of voting units or the distances between them (see section 3.2). Further, we show a rigorous justification for choosing a central map based on a committee voting scenario. Specifically, the central map is the one that minimizes the sum of distances from the maps voted on, similar to Kemeny ranking [Kemeny, 1959] (see Theorem 3.1).

En route to obtaining the medoid map we derive the *centroid* map which is not in fact a valid redistricting map, however has very interesting properties. Such as its (i, j) -entry being equal to the probability of the voting units i and j being in the same district. Moreover, we show a simple linear-time algorithm for obtaining this centroid map which we do not think is obvious given the fact that the structures we deal with are rather complicated (redistricting maps). Moreover, under the

¹These are not the truly uniform random samples from the immense and ill-defined space of all possible maps that we ideally want, but they are generally treated as such in courts.

assumption that we can sample valid maps in an independent and identically distributed manner, we derive the sample complexity for obtaining the centroid map.

Experimentally, we test our results over the states of North Carolina, Maryland, and Pennsylvania. Interestingly, we find that a by product of having a central map is a method for detecting gerrymandered maps. Concretely, the states of North Carolina and Pennsylvania have had enacted maps which were widely considered to be gerrymandered and in fact some were struck down by the state supreme court [LWV vs Commonwealth of Pennsylvania, 2018]. In response, some remedial maps were either suggested or enacted. We find that when we sample a large ensemble of redistricting maps and plot their distances from the centroid map, the gerrymandered maps have very large distances at the tail of the distribution whereas the remedial maps are much closer to the centroid. This perhaps suggests a new rule in drawing redistricting maps. Specifically, the drawn map should not be too faraway from the centroid.

2 Related Work

Less than a decade ago, several early works ushered in the current era of Markov Chain Monte Carlo (MCMC) sampling techniques for gerrymandering detection [Mattingly and Vaughn, 2014, Wu et al., 2015, Fifield et al., 2015]. Followup work has both refined these techniques and further analyzed their ability to approximate the target distribution. Authors of these works have been involved in court cases in Pennsylvania [Chikina et al., 2017] and North Carolina [Herschlag et al., 2020] with sampling approaches being used to demonstrate that existing maps were outliers as evidence of partisan gerrymandering. One of the most recent works in this area introduces the **ReCom** tool [DeFord et al., 2019] which will be used by the Wisconsin People’s Maps Commission and the Michigan Independent Citizens Redistricting Commission in the current redistricting cycle following the 2020 U.S. census [Chen, 2021]. Overall, these techniques have primarily been used to analyze and sometimes reject existing maps rather than draw new maps. However, we may think of them as at least narrowing the search space of maps drawn by legislatures. Along these lines, it has been shown that even the regulation of gerrymandering via outlier detection is subject to strategic manipulation [Brubach et al., 2020].

On the automated redistricting side, many map drawing algorithms have favored optimization approaches and in particular, optimizing some notion of compactness while avoiding explicit use of partisan information. Approaches emphasizing compactness include balanced power diagrams [Cohen-Addad et al., 2018], a k -median-based objective [Bycoffe et al., 2018], and minimizing the number of cut edges in a planar graph [Hettle et al., 2021]. Some works include partisan information for the sake of creating competitive districts (districts with narrow margins between the two main parties). The PEAR tool [Liu et al., 2016] balances nonpartisan criteria like compactness (defined by Polsby-Popper score [Polsby and Popper, 1991]) with other criteria such as competitiveness and uses an evolutionary algorithm with some similarity to the random walks taken by MCMC sampling approaches. Other works go even further in the explicitly partisan direction. For example, [Pegden et al., 2017] devises a game theoretic approach which aims to provide a map that is fair to the two dominant parties. Finally, there are methods which prefer simplicity such as the Splitline [Ryan and Smith, 2022] algorithm which iteratively splits a state until the desired number of districts is reached.

In all of these approaches the aim is to automate redistricting, but it is difficult to determine whether the choices made are the “right” or “fairest” decisions. The question of whether optimizing properties such as compactness while ignoring partisan factors could result in partisan bias has been a concern for some time. [Cho, 2019] notes a comment by Justice Scalia suggesting that

such a process could be biased against Democratic voters clustered in cities in *Vieth v. Jubelirer* [Vieth v. Jubelirer, 2004]. For those that do take partisan bias into account, there are questions of whether purposely drawing competitive districts or giving a fair allocation to two parties are really beneficial to voters.

Finally, like [Abrishami et al., 2020] we are introducing a distance measure over redistricting maps. However, our distance is easy to compute and does not require solving a linear program. Further, our focus is on the implications of having a distance measure, i.e. the medoid and centroid maps that will be introduced. Moreover, unlike [Abrishami et al., 2020] we can detect gerrymandered maps much more rigorously without using an embedding method and using 200,000 samples instead of only 100.

3 Problem Set-Up

A given state is modelled by a graph $G = (V, E)$ where each vertex $v \in V$ represents a voting block (*unit*). Each unit v has a weight $w(v) > 0$ which represents its population. Further, $\forall u, v \in V$ there is an edge $e = (u, v) \in E$ if and only if the two vertices are *connected* (geographically this means that the units u and v share a boundary). The number of units is $|V| = n$. A *redistricting* (*redistricting map* or simply *map*) M is a partition of V into $k > 0$ many districts, i.e., $V = V_1 \cup V_2 \cdots \cup V_k$ where each V_i represents a district and $\forall i \in [k], |V_i| \neq 0$ and $\forall i, j \in [k], V_i \cap V_j = \emptyset$. The redistricting map M is decided by the induced partition, i.e., $M = \{V_1, \dots, V_k\}$. For a redistricting M to be considered valid, it must satisfy a collection of properties, some of which are specific to the given state. We use the most common properties as stated in [DeFord et al., 2019, Hettle et al., 2021]:

1. *Compactness*: The given partitioning should have “compact” districts. Although there is no definitive mathematical criterion which decides compactness for districts, some have used common definitions such as Polsby-Popper or Reock Score [Alexeev and Nixon, 2018]. Others have used a clustering criterion like the k -median objective [Cohen-Addad et al., 2018] or considered the total number of cuts (number of edges between vertices in different districts) [DeFord et al., 2019].
2. *Equal Population*: To satisfy the desideratum of “one person one vote” each district should have approximately the same number of individuals. I.e., a given district V_i should satisfy $\sum_{v \in V_i} w(v) \in [(1 - \epsilon) \frac{\sum_{v \in V} w(v)}{k}, (1 + \epsilon) \frac{\sum_{v \in V} w(v)}{k}]$ where ϵ is a non-negative parameter relaxing the strict constraint of districts having exactly the same number of individuals.
3. *Contiguity*: Each district (partition) V_i should be a connected component, i.e., $\forall i \in [k]$ and $\forall u, v \in V_i$, v should be reachable from u through vertices which only belong to V_i .

Our proofs do not rely on these properties and therefore can likely even accommodate further desired properties.

Let \mathcal{M} be the set of all valid maps. Let $\mathcal{D}(\mathcal{M})$ be a distribution over these maps. Furthermore, define a distance function over the maps $d : \mathcal{M} \times \mathcal{M} \rightarrow [0, \infty]$. Then the *population medoid map* is M^* which is a solution to the following:

$$M^* = \arg \min_{M \in \mathcal{M}} \mathbb{E}_{M' \sim \mathcal{D}(\mathcal{M})} [d(M, M')] \quad (1)$$

In words, the population medoid map is a valid map minimizing the expected sum of distances away from all valid maps according to the distribution $\mathcal{D}(\mathcal{M})$. This serves as a natural way to define a central or typical map with respect to a given distance metric of interest.

Since we clearly operate over a sample (a finite collection) from $\mathcal{D}(\mathcal{M})$; therefore, we assume that the following condition holds:

Condition 3.1. *We can sample maps from the distribution $\mathcal{D}(\mathcal{M})$ in an independent and identically distributed (*iid*) manner in polynomial time.*

We note that although independence certainly does not hold over the sampling methods of [DeFord et al., 2019, Mattingly and Vaughn, 2014] since they use MCMC methods, it makes the derivations significantly more tractable. Further, the specific choice of the sampling technique is somewhat immaterial to our objective.

Based on the above condition, we can sample from the distribution \mathcal{M} efficiently and obtain a finite set of maps \mathcal{M}_T having T many maps, i.e., $|\mathcal{M}_T| = T$.

Now, we define the *sample medoid*, which is simply the extension of the population medoid, but restricted to the given sample. This leads to the following definition:

$$\bar{M}^* = \arg \min_{M \in \mathcal{M}_T} \sum_{M' \in \mathcal{M}_T} d(M, M') \quad (2)$$

3.1 Justification for Choosing a Central Map

Connection to the Kemeny Rule: We note that the Kemeny rule [Kemeny, 1959, Brandt et al., 2016] is the main inspiration behind our proposed framework. More specifically, if we have a set of alternatives and each individual votes by ranking the alternatives, then the Kemeny rule gives a method for aggregating the resulting collection of rankings. This is done by introducing a distance measure over rankings (the Kendall tau distance [Kendall, 1938]) and then choosing the ranking which minimizes the sum of distances away from the other rankings in the collection as the aggregate ranking.

Although we do not deal with rankings here, we follow a similar approach to the Kemeny rule as we introduce a distance measure over redistricting maps and choose the map which minimizes the sum of the distances as the aggregate map. In fact, recently there has been significant citizen engagement in drawing redistricting maps. For example, in the state of Maryland an executive order from the governor has established a web page to collect citizen submissions of redistricting maps [Commission, 2021]. If each member of a committee was to vote for exactly one map in the given submitted maps, then if we interpret the probability $p_{M'}$ for a map $M' \in \mathcal{M}$ to be the number of votes it received from the total set of votes, then the medoid map M^* (similar to the Kemeny ranking) would be the map which minimizes the weighted sum of distances from the set of maps voted on. We include this result as a theorem and its proof follows directly from the definition we gave above:

Theorem 3.1. *Suppose we have a committee of \mathcal{T} many voters and that each voter votes for one map from a subset of all possible valid maps \mathcal{M} , then given a map M' , if we assign it a probability $p_{M'} = \frac{\sum_{\tau=1}^{\mathcal{T}} v_{\tau, M'}}{\mathcal{T}}$ where $v_{\tau, M'} \in \{0, 1\}$ is the vote of member τ for map M' , then the medoid map $M^* = \arg \min_{M \in \mathcal{M}} \mathbb{E}_{M' \sim p_{M'}} [d(M, M')]$ is the map that minimizes the sum of distances from the set of valid maps where the distance to each map is weighted by the total votes it receives.*

Connection to Distance and Clustering Based Outlier Detection: The medoid map by virtue of minimizing the sum of distances can be considered a central map. Accordingly, one may consider using the medoid map to test for gerrymandering in a manner similar to distance and clustering based outlier detection [He et al., 2003, Knox and Ng, 1998]. More specifically, given a large ensemble of maps, if the enacted map is faraway from the medoid² in comparison to the

²In our experiments, we actually use the centroid instead of the medoid map.

ensemble then suggests possible gerrymandering. In fact, we carry experiments on the states of North Carolina and Pennsylvania (both of which have had enacted maps which were considered gerrymandered and struck down by the state supreme court) and we indeed find the gerrymandered maps to be faraway whereas the remedial maps are much closer in terms distance.

3.2 Distance over Redistricting Maps

Before we introduce a distance over maps, we note that a given map (partition) M can be represented using an “adjacency” matrix A in which $A(i, j) = 1$ if and only if $\exists V_\ell \in M : i, j \in V_\ell$ otherwise $A(i, j) = 0$. We note that this adjacency matrix can be seen as drawing an edge between every two vertices i, j in the same partition, i.e., where $A(i, j) = 1$. It is clear that we can refer to a map by the partition M or the induced adjacency matrix A . Accordingly, we refer to the population medoid as M^* or A^* and the sample medoid as \bar{M}^* or \bar{A}^* .

We now introduce our distance family which is parametrized by a weight matrix Θ and have the following form:

$$d_\Theta(A_1, A_2) = \frac{1}{2} \sum_{i, j \in V} \theta(i, j) |A_1(i, j) - A_2(i, j)| \quad (3)$$

where we only require that $\theta(i, j) > 0, \forall i, j \in V$. For the simple case where $\theta(i, j) = 1, \forall i, j \in V$, our distance $d_1(A_1, A_2)$ is equivalent to a Hamming distance over adjacency matrices and therefore has an edit distance interpretation. If we were to draw edges between vertices according to the entries with 1 in A_1 , then $d_1(A_1, A_2)$ simply equals the number of edges that must be added/deleted to obtain A_2 . We refer to the metric $d_1(., .)$ as the *uniform distance*. We note that such a distance measure was considered in previous work that considered adversarial attacks on clustering [Chhabra et al., 2020, Cinà et al., 2022].

Another choice of Θ that leads to a meaningful metric is the *population-weighted distance* where $\theta(i, j) = w(i)w(j)$. This leads to $d_W(A_1, A_2) = \frac{1}{2} \sum_{i, j \in V} w(i)w(j) |A_1(i, j) - A_2(i, j)|$. The population-weighted distance takes into account the number of individuals being separated from one another when vertices i and j are separated from one another³ by assigning a cost of $w(i)w(j)$. By contrast, the uniform distance assigns the same cost regardless of the population values and thus has a uniform weight over the separation of units immaterial of the populations which they include.

Another choice of metric which is meaningful, could be of the form $\theta(i, j) = f(l(i, j))$ where $l(i, j)$ is the length of a shortest path between i and j and $f(.)$ is a positive decreasing function such as $f(l(i, j)) = e^{-l(i, j)}$. Such a metric would place a smaller penalty for separating vertices that are far away from each other.

4 Algorithms

We show our linear time algorithm for obtaining the sample medoid in subsection 4.1. In 4.2 we define the population centroid, derive sample complexity guarantees for obtaining it, and show that its (i, j) entry equals the probability of having i and j in the same district. Finally, in 4.3 we discuss obtaining the population medoid. Specifically, we show that even for a simple one dimensional distribution an arbitrarily large sample is not sufficient for obtaining the population medoid. However, we introduce a simple assumption on the distribution under which the sample medoid would be a good estimate of the population medoid.

³Recall that each vertex (unit) is a voting block (AKA voter tabulation district) and units may contain different numbers of voters.

Algorithm 1 Finding the Sample Medoid

Input: $\mathcal{M}_T = \{A_1, \dots, A_T\}$, $\Theta = \{\theta(i, j) > 0, \forall i, j \in V\}$.

1: Calculate the centroid map $\bar{A}_c = \frac{1}{T} \sum_{t=1}^T A_t$.

2: Pick the map $\bar{A}^* \in \mathcal{M}_T$ which minimizes the $d_{2,\Theta}$ distance from the centroid \bar{A}_c , i.e. $\bar{A}^* = \arg \min_{A \in \mathcal{M}_T} d_{2,\Theta}(A, \bar{A}_c)$.

return \bar{A}^*

First, before we introduce our algorithms we show that our distance family is indeed a metric, i.e. satisfies the properties of a metric:

Theorem 4.1. *For all Θ such that $\forall i, j, \theta(i, j) > 0$, the following distance function is a metric.*

$$d_{\Theta}(A_1, A_2) = \frac{1}{2} \sum_{i,j \in V} \theta(i, j) |A_1(i, j) - A_2(i, j)|$$

4.1 Obtaining the Sample Medoid

We note that in general obtaining the sample medoid is not scalable since it usually takes quadratic time [Newling and Fleuret, 2017] in the number of samples, i.e. $O(T^2)$. An $O(T^2)$ run time can be easily obtained through a brute-force algorithm which for every map calculates the sum of the distances from other maps and then selects the map with the minimum sum. However, for our family of distances $d_{\Theta}(\cdot, \cdot)$ we show that the medoid map is the closest map to the centroid map and show a simple algorithm that runs in $O(T)$ time for obtaining the sample medoid. The fundamental cause behind this speed up is an equivalence between the Hamming distance over binary vectors and the square of the Euclidean distance which is still maintained with our generalized distance. More specifically given two matrices A_1, A_2 , then we can define $d_{2,\Theta}(A_1, A_2) = \frac{1}{2} \sum_{i,j \in V} \theta(i, j) (A_1(i, j) - A_2(i, j))^2$, clearly if matrices A_1, A_2 are binary then $d_{2,\Theta}(A_1, A_2) = d_{\Theta}(A_1, A_2)$. However, that would not be the case if one of them had fractional entries. We can obtain the following decomposition theorem:

Theorem 4.2. *Given a collection of redistricting maps A_1, \dots, A_T , the sum of distances of the maps away from a fixed redistricting map A' equals the following:*

$$\sum_{t=1}^T d_{\Theta}(A_t, A') = \sum_{t=1}^T d_{2,\Theta}(A_t, \bar{A}_c) + T d_{2,\Theta}(\bar{A}_c, A') \quad (4)$$

where $\bar{A}_c = \frac{1}{T} \sum_{t=1}^T A_t$.

Notice that the above theorem introduces the centroid map \bar{A}_c which is simply equal to the empirical mean of the adjacency maps. It should be clear that with the exception of trivial cases the centroid map \bar{A}_c is not a valid adjacency matrix, since despite being symmetric it would have fractional entries between 0 and 1. Hence, the centroid map also does not lead to a valid partition or districting. Moreover, we note that it is more accurate to call \bar{A}_c the sample centroid, as apposed to the population centroid A_c (see section 4.2) which we would obtain with an infinite number of samples.

The above theorem leads to the following algorithm:

Theorem 4.3. *Algorithm 1 returns the correct sample medoid and runs in time linear in the number of samples T .*

Proof. We start by showing the correctness. We note that the sample medoid is obtained from the set of sampled maps A_1, \dots, A_T . Therefore, referring to Eq (4) we are looking for $A' \in \{A_1, \dots, A_T\}$ that minimizes $\sum_{t=1}^T d_\Theta(A_t, A')$. Now, from Eq (4) it is clear that, the first term is constant and independent of our choice of A' whereas the second is minimized by picking the map A' that minimizes the distance $d_{2,\Theta}(\bar{A}_c, A')$. It follows that algorithm 1 is correct, since in the first step it finds \bar{A}_c and in the second it finds the sampled mapped closest to \bar{A}_c in terms of the distance $d_{2,\Theta}$.

Since calculating the centroid in step 1 takes $O(T)$ time and finding the closest map in \mathcal{M}_T also takes $O(T)$ time, it follows that the run time is indeed $O(T)$. \square

We note that calculating the sample medoid in algorithm 1 has no dependence on the generating method. Therefore, if a set of maps are produced through any mechanism and are considered to be representative and sufficiently diverse, then algorithm 1 can be used to obtain the sample medoid in time that is linear in the number of samples.

4.2 Sample Complexity for Obtaining the Population Centroid

In the previous section we introduced the sample centroid \bar{A}_c which is simply equal to the empirical mean that we get by taking the average of the adjacency matrices, i.e. $\bar{A}_c = \frac{1}{T} \sum_{t=1}^T A_t$. We now consider the population centroid $A_c = \lim_{T \rightarrow \infty} \bar{A}_c$. Clearly, by the law of large numbers [Zubrzycki, 1972], we have $A_c(i, j) = \mathbb{E}[A(i, j)]$. It is also clear that A_c has an interesting property, specifically the (i, j) -entry equals the probability that i and j are in the same district:

Theorem 4.4. $A_c(i, j) = \Pr[i \text{ and } j \text{ in the same district}]$.

Now we show that with a sufficient number of samples, the entries of the sample centroid are close to the population centroid. Specifically, we have the following theorem:

Theorem 4.5. *If we sample $T = \frac{1}{\epsilon^2} \ln \frac{n}{\delta}$ iid samples, then with probability at least $1 - \delta$, we have that $\forall i, j \in V : |\bar{A}_c(i, j) - A_c(i, j)| \leq \epsilon$.*

We also bound the $d_{2,\Theta}$ value between \bar{A}_c and A_c :

Theorem 4.6. *Let $\max_{i,j \in V} \sqrt{\theta(i, j)} = \rho$, if we have $T = \frac{\rho n^2}{\epsilon^2} \ln \frac{n}{\delta}$ iid samples, then $d_{2,\Theta}(\bar{A}_c, A_c) \leq \epsilon$ with probability at least $1 - \delta$.*

4.3 Obtaining the Population Medoid

Having found the sample centroid \bar{A}_c and shown that it is a good estimate of the population centroid A_c , we now show that we can obtain a good estimate of the population medoid by solving an optimization problem. Specifically, assuming that we have the population centroid A_c , then the population medoid is simply a valid redistricting map A which has a minimum $d_{2,\Theta}(A, A_c)$ value. This follows immediately from Theorem 4.2. More interestingly, we show in fact that this optimization problem is a constrained instance of the min k -cut problem:

Theorem 4.7. *Given the population centroid A_c , the population medoid A^* can be obtained by solving a constrained min k -cut problem.*

If we have a good estimate \bar{A}_c of the population centroid A_c , then we can solve the above optimization using \bar{A}_c instead of A_c and obtain an estimate of the population medoid \bar{A}^* instead of the true population medoid A^* and bound the error of that estimate. The issue is that the min k -cut problem is NP-hard [Saran and Vazirani, 1995] and while there are approximation algorithms for it,

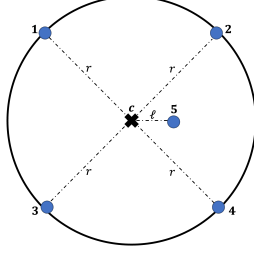


Figure 1: Points 1,2,3, and 4 all lie on the circle and the angle between any two adjacent points is 90° . Point 5 is a distance ℓ from the circle center c .

the additional constraints on the partition being a valid redistricting (each partition being contiguous, of equal population, and compact) make it quite difficult to approximate the objective. In fact, excluding the objective and focusing on the constraint alone, only the work of [Hettle et al., 2021] has produced approximation algorithm for redistricting maps but has done that for the restricted case of grid graphs. Further, while there exists heuristics for solving the min k -cut for redistricting maps they only scale to at most around 500 vertices [Validi and Buchanan, 2022].

Having shown the difficulty in obtaining the population medoid by solving an optimization problem, it is reasonable to wonder whether we can gain any guarantees about the population medoid by sampling. We show a negative result. Specifically, we show that in general we cannot guarantee that we can estimate the sample medoid of a distribution with high probability by choosing a sampled map even if we sample an arbitrarily large number of samples despite the fact that we can easily estimate the centroid (expected) value. This can in fact be shown with an example of a 2-dimensional random variable as demonstrated in the theorem below. In Appendix A we prove this over redistricting map with a longer and more elaborate proof:

Theorem 4.8. *There exists a distribution over points in the 2-dimensional space for which the expected value can be estimated to an arbitrary error ϵ with a polynomial number of **iid** samples. However, by only selecting a sampled point we cannot: (1) Obtain a point that is arbitrarily close to the medoid. (2) Obtain a point whose medoid cost function value is arbitrarily close to the minimum cost function value.*

Proof. Consider the set of points shown in Figure 1. Specifically, points x_1, x_2, x_3 and x_4 lie on a circle of radius r at an equal separation. Point x_5 lie closer to the center of the circle c at a distance of ℓ . Further, each point x_i has a probability p_i of being sampled. Specifically, $p_5 = \delta > 0$ and $p_1 = p_2 = p_3 = p_4 = \frac{1-\delta}{4}$. The measure of distance we use is the Euclidean distance.

The centroid of the distribution is the expected value, i.e. $\mathbb{E}[x] = \sum_{j=1}^5 p_j x_j$. It is straightforward to show that given **iid** samples $\{\hat{x}_1, \hat{x}_2, \dots, \hat{x}_T\}$ where $T = \Omega(\frac{\log(1/\rho)}{\epsilon})$, then $\left\| \frac{1}{T} \sum_{t=1}^T \hat{x}_t - \mathbb{E}[x] \right\|_2^2 \leq r^2 \epsilon$ with probability at least $1 - \rho$. This follows by applying the generalized Hoeffding inequality (see [Ashtiani et al., 2016] for example). Therefore the centroid can be estimated using a polynomial number of samples.

Now, given a candidate medoid point x' , the cost function is $f(x') = \sum_{j=1}^5 p_j d(x', x_j)$. Note that the medoid is the value of x' which minimizes $f(x')$ and also x' must be a valid point, i.e. $x' \in \{x_1, x_2, x_3, x_4, x_5\}$. It is easy to verify that $f(x_1) = \frac{1-\delta}{4} [d(x_1, x_2) + d(x_1, x_3) + d(x_1, x_4)] + \delta d(x_1, x_5) > \frac{1-\delta}{4} [0 + 2\sqrt{2}r + 2r] = \frac{1-\delta}{2} (1 + \sqrt{2})r$. By symmetry it also follows that $f(x_2), f(x_3), f(x_4)$ are each lower bounded by $\frac{1-\delta}{2} (1 + \sqrt{2})r$.

On the other hand, we have $f(x_5) = \frac{1-\delta}{4} \sum_{j=1}^4 d(x_5, x_j) \leq \frac{1-\delta}{4} \sum_{j=1}^4 [d(x_5, c) + d(c, x_j)] \leq$

$\frac{1-\delta}{4}(4(r+\ell)) = (1-\delta)(r+\ell)$. Further, for any $i \neq 5$: $\frac{f(x_i)}{f(x_5)} \geq \frac{\frac{1-\delta}{2}(1+\sqrt{2})r}{(1-\delta)(r+\ell)} = \frac{(1+\sqrt{2})}{2(1+\frac{1}{1000})} > 1.2$ by setting $\ell = \frac{1}{1000}r$, and therefore x_5 is the medoid. Further, $\forall i \in \{1, 2, 3, 4\} : d(x_i, x_5) \geq d(x_i, c) - d(c, x_5) \geq r - \ell \geq 0.999r$. Therefore, if we do not sample x_5 , then we can neither obtain a point that is arbitrarily close to the medoid (1) or obtain a point whose medoid cost function is arbitrarily close to the minimum medoid cost function (2). Given T many **iid** samples, let the probability of sampling point x_5 be ρ , then we can show the following:

$$\begin{aligned}
& \Pr[\text{Sampling } x_5 \text{ in } T \text{ iid samples}] \\
&= 1 - \Pr[\text{Not sampling } x_5 \text{ in } T \text{ iid samples}] \\
&= 1 - (1 - \delta)^T = \rho \\
&\iff \delta = 1 - \sqrt[T]{1 - \rho}
\end{aligned}$$

Therefore for any arbitrarily small probability ρ , there is a value δ for sampling x_5 and therefore a distribution where x_5 (the medoid) is sampled with a vanishingly small probability. This proves (1) and (2). \square

We therefore, use a heuristic to find the medoid as mentioned in section 5.

5 Experiments

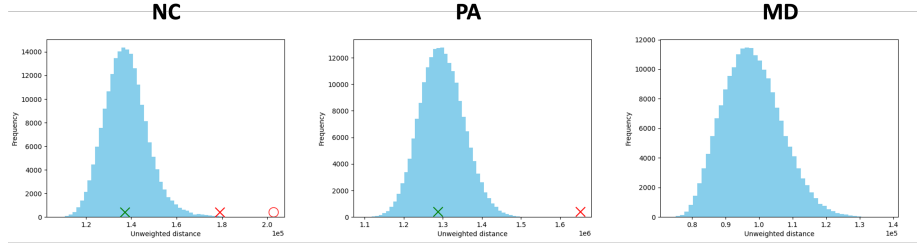


Figure 2: Distance histograms for NC (left), PA (middle), and MD (right) using the unweighted distance measure. For NC and PA the distances of gerrymandered maps are indicated with red markers whereas the distances of the remedial maps are indicated with green markers (for NC the \circ and the \times are for 2011 and 2016 enacted maps, respectively).

We conduct our experiments over 3 states. Specifically, North Carolina (NC), Maryland (MD), and Pennsylvania’s (PA). The number of voting units (vertices) and districts are around 2,700, 1,800, and 8,900 for NC, MD, and PA, respectively. Further, the number of districts are 13, 8, and 18 for NC, MD, and PA, respectively⁴. Accordingly, PA is the largest state whereas MD is the smallest. To generate a collection of maps, we use the Recombination algorithm **ReCom** from [DeFord et al., 2019] whose implementation is available online. We note that **ReCom** is a Markov Chain Monte Carlo (MCMC) sampling method and hence the generated samples are not actually **iid**. While this means that Condition (3.1) does not hold, we believe that our theorems still have utility and that future work can address more realistic sampling conditions. Moreover, we always exclude

⁴Note that for PA the number of districts has been reduced by one to 17 districts after the 2020 census. However, since we use past election results we have 18 districts.

the first 2,000 from any calculation as these are considered to be “burn-in” samples⁵. Throughout this section when we say distance we mean $d_{2,\Theta}(\cdot, \cdot)$ instead of $d_\Theta(\cdot, \cdot)$. We also note that further experimental results are included in Appendix B.

Convergence of the Centroid: We note that previous work such as [DeFord et al., 2019, DeFord and Duchin, 2019] had used the **ReCom** algorithm for estimating statistics such as the histogram of election seats won by a party and has noted that using 50,000 samples is sufficient for accurate results. However, our setting is more challenging. Specifically, the centroid includes $\Omega(n^2)$ entries where n is the total number of voting units (vertices) whereas the election histogram includes only k entries where k is the number of districts and usually orders of magnitude smaller than the number of voting units. We sample 200,000 maps instead to estimate the centroid. Here we emphasize the importance of our linear-time algorithm since using a quadratic-time algorithm on samples of the order of even 50,000 could be forbidding. Following similar practice to [Herschlag et al., 2020] for verifying convergence, we repeat the procedure (sampling using **ReCom** and estimating the centroid) for a total of three times for each state where we start from a different seed map each time and verify that all three runs result in essentially the same centroid estimate.

To verify the closeness of the different centroid estimates, we calculate the distances between them and compare them to their distances from sampled redistricting maps using **ReCom**. We find that the centroids are orders of magnitude closer to each other than to any other sampled map. For example, for PA the maximum unweighted distance between any two centroids is less than 2.28×10^3 whereas the minimum unweighted distance between any of the three centroids and any sampled map is around 1.1×10^6 which is three orders of magnitude higher. Similarly, for NC the maximum weighted distance between any two centroids is around 1.12×10^9 whereas the minimum weighted distance between any of the three centroids and any sampled map is around 1.37×10^{12} which is again three orders of magnitude higher. We include more results on the distance between the centroids as well as the distance histograms for each centroid in the Appendix B and we find that the results from different runs are essentially in agreement.

Distance Histogram and Detecting Gerrymandered Maps: For each state we plot the distance histogram from its centroid. More specifically, having estimated the centroid \bar{A}_c , we sample 200,000 maps and calculate $d_{2,\Theta}(\bar{A}_c, A_t)$ where A_t is the t^{th} sampled map. Figure 2 shows the unweighted distance histogram. The histogram appears like a normal distribution peaking at the middle (around the mean) and falling almost symmetrically away from the middle. This also indicates that while the centroid minimizes the sum of $d_{2,\Theta}(\bar{A}_c, A_t)$ distances, the maps do not actually concentrate around it as otherwise the histogram would have had a peak in the beginning at small distance values. Interestingly, the histogram has a similar shape for all three states (NC, MD, PA). Further, this shape of the histogram remains largely unchanged for the weighted-distance measure.

Furthermore, previous work has used similar sampling methods to detect gerrymandered maps [Chikina et al., 2017, Mattingly and Vaughn, 2014, Herschlag et al., 2020]. In essence these paper demonstrate that the election outcome achieved by the enacted map is rare to happen in comparison to the large sampled ensemble of redistricting maps. Using similar logic, we find that we can also detect gerrymandered maps. Specifically, the 2011 and 2016 enacted maps of NC were widely considered to be gerrymandered and we find both maps to be at the right tail of the histogram and very faraway from the centroid. In contrast, to a remedial NC map that was drawn by a set

⁵In MCMC, the chain is supposed to converge to a stationary distribution after some number of steps. These number of steps are called the “mixing time”. Although for **ReCom** the mixing time has not been theoretically calculated, empirically it seems that 2,000 steps are sufficient.

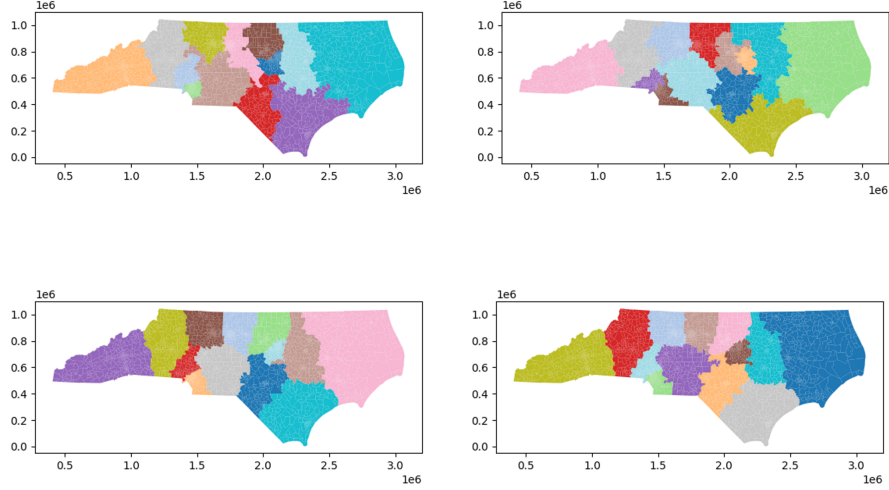


Figure 3: NC medoids, the left column shows maps from one run and the right column from another. Top row: A_{closest} , Bottom row: \hat{A}^* .

of retired judges [Herschlag et al., 2020] which is much closer to the centroid (see Figure 2 red and green marked points). Similarly, in the case of PA the 2011 enacted map was in fact struck down by the PA supreme court and a remedial map was drawn. We again find similar observations in the case of PA with the gerrymandered map being faraway and the remedial map being much closer the centroid.

This suggests that we indeed have a method for detecting gerrymandered maps that in comparison to previous methods has the advantage of not needing election results (only a reasonable distance measure) and is very interpretable. Further, it is reasonable to consider this as setting a new rule when drawing redistricting maps or at least a guideline for drawing redistricting maps in practice: the drawn map should not be very faraway from the centroid. In Appendix B we show the histogram for weighted distance measure and using other centroids and see that they lead to the same observations (including gerrymandering detection).

Finding the medoid: We discuss the results for NC and the unweighted distance. Since we have shown in subsection 4.3 that the medoid cannot be obtained by sampling, we follow a heuristic that consists of these steps: (1) Sample 200,000 maps and pick the one closest to the centroid A_{closest} . (2) Start the **ReCom** chain from A_{closest} but given a specific state (redistricting map) we only allow transitions to new states (maps) that are closer to the centroid and we do this for a total of 200,000 steps to obtain the final estimated medoid \hat{A}^* . We follow this procedure three times one for each centroid ⁶. Figure 3 (top row) shows the A_{closest} medoids from two different runs (each comparing to a different centroid). It is not difficult to see that they are different. The bottom row shows the final medoids after we run the chain from A_{closest} to obtain \hat{A}^* . We see that the final medoids are indeed very similar and in fact when we measure the distances between them we find them to be very close.

It is worthwhile to wonder about the election results obtained when using the final medoids. We find that all estimated medoids lead to the same election results and equal or close to the peak of the election histogram: 5 and 4 using governor and senate votes in the 2016 election, respectively. See Figure 4. Further, results on finding the medoid are discussed in Appendix B.

⁶As mentioned before we get three centroids each from sampling a chain that starts with a different seed.

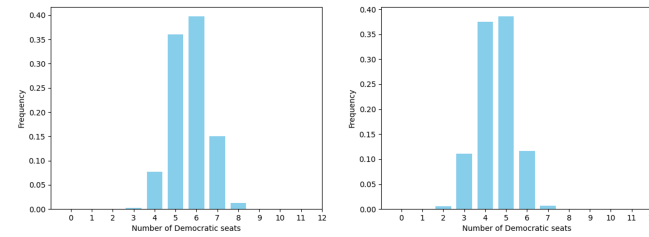


Figure 4: Number of Democratic seats won: left: Governor Votes in 2016, right: Senate Votes in 2016.

References

- [Abrishami et al., 2020] Abrishami, T., Guillen, N., Rule, P., Schutzman, Z., Solomon, J., Weighill, T., and Wu, S. (2020). Geometry of graph partitions via optimal transport. *SIAM Journal on Scientific Computing*, 42(5):A3340–A3366.
- [Alexeev and Mixon, 2018] Alexeev, B. and Mixon, D. G. (2018). An impossibility theorem for gerrymandering. *The American Mathematical Monthly*, 125:878–884.
- [Ashtiani et al., 2016] Ashtiani, H., Kushagra, S., and Ben-David, S. (2016). Clustering with same-cluster queries. *Advances in neural information processing systems*, 29.
- [Brandt et al., 2016] Brandt, F., Conitzer, V., Endriss, U., Lang, J., and Procaccia, A. D. (2016). *Handbook of computational social choice*. Cambridge University Press.
- [Brubach et al., 2020] Brubach, B., Srinivasan, A., and Zhao, S. (2020). Meddling metrics: the effects of measuring and constraining partisan gerrymandering on voter incentives. In *Proceedings of the 21st ACM Conference on Economics and Computation*, pages 815–833.
- [Bycoffe et al., 2018] Bycoffe, A., Koeze, E., Wasserman, D., and Wolfe, J. (2018). The Atlas Of Redistricting. <https://projects.fivethirtyeight.com/redistricting-maps/>. [Online; published 25-January-2018; accessed 15-August-2019].
- [Chen, 2021] Chen, M. (2021). Tufts research lab aids states with redistricting process. *The Tufts Daily*.
- [Chhabra et al., 2020] Chhabra, A., Roy, A., and Mohapatra, P. (2020). Suspicion-free adversarial attacks on clustering algorithms. In *Proceedings of the AAAI Conference on Artificial Intelligence*, volume 34, pages 3625–3632.
- [Chikina et al., 2017] Chikina, M., Frieze, A., and Pegden, W. (2017). Assessing significance in a markov chain without mixing. *Proceedings of the National Academy of Sciences*, 114(11):2860–2864.
- [Cho, 2019] Cho, W. K. T. (2019). Technology-enabled coin flips for judging partisan gerrymandering. *Southern California law review*, 93.
- [Cinà et al., 2022] Cinà, A. E., Torcinovich, A., and Pelillo, M. (2022). A black-box adversarial attack for poisoning clustering. *Pattern Recognition*, 122:108306.

- [Cohen-Addad et al., 2018] Cohen-Addad, V., Klein, P. N., and Young, N. E. (2018). Balanced centroidal power diagrams for redistricting. In *Proceedings of the 26th ACM SIGSPATIAL International Conference on Advances in Geographic Information Systems*, pages 389–396.
- [Commission, 2021] Commission, M. C. R. (2021). Redistricting Map Submission Process. <https://redistricting.maryland.gov/Pages/plan-proposals.aspx>. [Online; accessed 20-October-2021].
- [DeFord and Duchin, 2019] DeFord, D. and Duchin, M. (2019). Redistricting reform in virginia: Districting criteria in context. *Virginia Policy Review*, 12(2):120–146.
- [DeFord et al., 2019] DeFord, D., Duchin, M., and Solomon, J. (2019). Recombination: A family of markov chains for redistricting. *arXiv preprint arXiv:1911.05725*.
- [Fifield et al., 2015] Fifield, B., Higgins, M., Imai, K., and Tarr, A. (2015). A new automated redistricting simulator using markov chain monte carlo. *Work. Pap., Princeton Univ., Princeton, NJ*.
- [He et al., 2003] He, Z., Xu, X., and Deng, S. (2003). Discovering cluster-based local outliers. *Pattern recognition letters*, 24(9-10):1641–1650.
- [Herschlag et al., 2020] Herschlag, G., Kang, H. S., Luo, J., Graves, C. V., Bangia, S., Ravier, R., and Mattingly, J. C. (2020). Quantifying gerrymandering in north carolina. *Statistics and Public Policy*, 7(1):30–38.
- [Hettle et al., 2021] Hettle, C., Zhu, S., Gupta, S., and Xie, Y. (2021). Balanced districting on grid graphs with provable compactness and contiguity. *arXiv preprint arXiv:2102.05028*.
- [Kemeny, 1959] Kemeny, J. G. (1959). Mathematics without numbers. *Daedalus*, 88(4):577–591.
- [Kendall, 1938] Kendall, M. G. (1938). A new measure of rank correlation. *Biometrika*, 30(1/2):81–93.
- [Knox and Ng, 1998] Knox, E. M. and Ng, R. T. (1998). Algorithms for mining distancebased outliers in large datasets. In *Proceedings of the international conference on very large data bases*, pages 392–403. Citeseer.
- [Liu et al., 2016] Liu, Y. Y., Cho, W. K. T., and Wang, S. (2016). Pear: a massively parallel evolutionary computation approach for political redistricting optimization and analysis. *Swarm and Evolutionary Computation*, 30:78 – 92.
- [LWV vs Commonwealth of Pennsylvania, 2018] LWV vs Commonwealth of Pennsylvania (No. 159 MM (2018)).
- [Mattingly and Vaughn, 2014] Mattingly, J. C. and Vaughn, C. (2014). Redistricting and the will of the people. *arXiv preprint arXiv:1410.8796*.
- [Newling and Fleuret, 2017] Newling, J. and Fleuret, F. (2017). A sub-quadratic exact medoid algorithm. In *Artificial Intelligence and Statistics*, pages 185–193. PMLR.
- [Pegden et al., 2017] Pegden, W., Procaccia, A. D., and Yu, D. (2017). A partisan districting protocol with provably nonpartisan outcomes. *arXiv preprint arXiv:1710.08781*.

- [Polsby and Popper, 1991] Polsby, D. D. and Popper, R. D. (1991). The third criterion: Compactness as a procedural safeguard against partisan gerrymandering. *Yale Law & Policy Review*, 9(2):301–353.
- [Rucho v. Common Cause, 2019] Rucho v. Common Cause (No. 18-422, 588 U.S. ____ (2019)).
- [Ryan and Smith, 2022] Ryan, I. and Smith, W. D. (2022). Splitline districtings of all 50 states + DC + PR. <https://rangevoting.org/SplitLR.html>. [Online; accessed 15-August-2019].
- [Saran and Vazirani, 1995] Saran, H. and Vazirani, V. V. (1995). Finding k cuts within twice the optimal. *SIAM Journal on Computing*, 24(1):101–108.
- [Validi and Buchanan, 2022] Validi, H. and Buchanan, A. (2022). Political districting to minimize cut edges. *Mathematical Programming Computation*, pages 1–50.
- [Vieth v. Jubelirer, 2004] Vieth v. Jubelirer (No. 02-1580, 541 U.S. 267 (2004)).
- [Wu et al., 2015] Wu, L. C., Dou, J. X., Sleator, D., Frieze, A., and Miller, D. (2015). Impartial redistricting: A markov chain approach. *arXiv preprint arXiv:1510.03247*.
- [Zubrzycki, 1972] Zubrzycki, S. (1972). *Lectures in probability theory and mathematical statistics*, volume 38. Elsevier Publishing Company.

A Omitted Proofs

We restate the theorem and give its proof:

Theorem 3.1. *Suppose we have a committee of \mathcal{T} many voters and that each voter votes for one map from a subset of all possible valid maps \mathcal{M} , then given a map M' , if we assign it a probability $p_{M'} = \frac{\sum_{\tau=1}^{\mathcal{T}} v_{\tau, M'}}{\mathcal{T}}$ where $v_{\tau, M'} \in \{0, 1\}$ is the vote of member τ for map M' , then the medoid map $M^* = \arg \min_{M \in \mathcal{M}} \mathbb{E}_{M' \sim p_{M'}} [d(M, M')]$ is the map that minimizes the sum of distances from the set of valid maps where the distance to each map is weighted by the total votes it receives.*

Proof. By definition of the weighted sum of distances for a map M from the set of all maps as:

$$\begin{aligned} M^* &= \arg \min_{M \in \mathcal{M}} \sum_{M' \in \mathcal{M}} \left[\left(\sum_{\tau} v_{\tau, M'} \right) d(M, M') \right] \\ &= \arg \min_{M \in \mathcal{M}} \sum_{M' \in \mathcal{M}} \left[\left(\frac{\sum_{\tau} v_{\tau, M'}}{\mathcal{T}} \right) d(M, M') \right] \\ &= \arg \min_{M \in \mathcal{M}} \sum_{M' \in \mathcal{M}} \left[p_{M'} d(M, M') \right] \\ &= \mathbb{E}_{M' \sim p_{M'}} [d(M, M')] \end{aligned}$$

□

We restate the next theorem and give its proof:

Theorem 4.1. *For all Θ such that $\forall i, j, \theta(i, j) > 0$, the following distance function is a metric.*

$$d_{\Theta}(A_1, A_2) = \frac{1}{2} \sum_{i, j \in V} \theta(i, j) |A_1(i, j) - A_2(i, j)|$$

Proof. Since $\theta(i, j) > 0, \forall i, j \in V$, it is clear that $d_{\Theta}(A_1, A_2)$ is non-negative, symmetric, and that it equals zero if and only if $A_1 = A_2$. The triangle inequality follows since $|A_1(i, j) - A_2(i, j)| = |A_1(i, j) - A_3(i, j) + A_3(i, j) - A_2(i, j)| \leq |A_1(i, j) - A_3(i, j)| + |A_3(i, j) - A_2(i, j)|$, therefore we have:

$$\begin{aligned} d_{\Theta}(A_1, A_2) &= \frac{1}{2} \sum_{i, j \in V} \theta(i, j) |A_1(i, j) - A_2(i, j)| \\ &\leq \frac{1}{2} \sum_{i, j \in V} \theta(i, j) (|A_1(i, j) - A_3(i, j)| + |A_3(i, j) - A_2(i, j)|) \\ &\leq \frac{1}{2} \sum_{i, j \in V} \theta(i, j) |A_1(i, j) - A_3(i, j)| \\ &\quad + \frac{1}{2} \sum_{i, j \in V} \theta(i, j) |A_3(i, j) - A_2(i, j)| \\ &= d_{\Theta}(A_1, A_3) + d_{\Theta}(A_2, A_3) \end{aligned}$$

□

We restate the next theorem and give its proof:

Theorem 4.2. *Given a collection of redistricting maps A_1, \dots, A_T , the sum of distances of the maps away from a fixed redistricting map A' equals the following:*

$$\sum_{t=1}^T d_{\Theta}(A_t, A') = \sum_{t=1}^T d_{2,\Theta}(A_t, \bar{A}_c) + T d_{2,\Theta}(\bar{A}_c, A') \quad (4)$$

where $\bar{A}_c = \frac{1}{T} \sum_{t=1}^T A_t$.

Proof. We begin with the following lemma:

Lemma 1. *For any A_1, A_2 that are binary matrices (entries either 0 or 1), with $d_{2,\Theta}(A_1, A_2) = \frac{1}{2} \sum_{i,j \in V} \theta(i,j)(A_1(i,j) - A_2(i,j))^2$, then we have that $d_{\Theta}(A_1, A_2) = d_{2,\Theta}(A_1, A_2)$.*

Proof. The proof immediately follows by observing that since A_1 and A_2 are binary it follows that $\forall i, j : |A_1(i,j) - A_2(i,j)| = (A_1(i,j) - A_2(i,j))^2$. I.e., it suffices to show that $|1 - 1| = |0 - 0| = (1 - 1)^2 = (0 - 0)^2 = 0$ and that $|1 - 0| = |0 - 1| = (1 - 0)^2 = (0 - 1)^2 = 1$. This leads to us being able to replace absolutes with squares and hence $d_{\Theta}(A_1, A_2) = d_{2,\Theta}(A_1, A_2)$. \square

It may seem redundant to introduce a new definition $d_{2,\Theta}(\cdot, \cdot)$ since by Lemma (1), they are equivalent. However, we will shortly be using $d_{2,\Theta}(\cdot, \cdot)$ over matrices which are not necessarily binary, clearly then we might have $d_{\Theta}(A_1, A_2) \neq d_{2,\Theta}(A_1, A_2)$.

We then introduce next lemma:

Lemma 2. *For any two matrices (not necessarily binary), the following holds:*

$$d_{2,\Theta}(A_1, A_2) = \frac{1}{2} \|A_1^{\Theta} - A_2^{\Theta}\|_2^2 \quad (5)$$

where $A_s^{\Theta}(i, j) = \sqrt{\theta(i, j)} A_s(i, j), \forall s \in \{0, 1\}$ and $\|A_1^{\Theta} - A_2^{\Theta}\|_2^2$ is the square of the ℓ_2 -norm of the vectorized form of the matrix $(A_1^{\Theta} - A_2^{\Theta})$.

Proof.

$$\begin{aligned} d_{2,\Theta}(A_1, A_2) &= \frac{1}{2} \sum_{i,j \in V} \theta(i, j) (A_1(i, j) - A_2(i, j))^2 \\ &= \frac{1}{2} \sum_{i,j \in V} (\sqrt{\theta(i, j)} A_1(i, j) - \sqrt{\theta(i, j)} A_2(i, j))^2 \\ &= \frac{1}{2} \|A_1^{\Theta} - A_2^{\Theta}\|_2^2 \end{aligned}$$

\square

With the lemmas above, we can now proof the decomposition theorem:

$$\begin{aligned}
\sum_{t=1}^T d_{\Theta}(A_t, A') &= \sum_{t=1}^T d_{2,\Theta}(A_t, A') \quad (\text{using Lemma 1}) \\
&= \sum_{t=1}^T \frac{1}{2} \|A_t^{\Theta} - A'^{\Theta}\|_2^2 \quad (\text{using Lemma 2}) \\
&= \frac{1}{2} \sum_{t=1}^T \|A_t^{\Theta} - \bar{A}_c^{\Theta} + \bar{A}_c^{\Theta} - A'^{\Theta}\|_2^2 \\
&= \frac{1}{2} \sum_{t=1}^T \left[(A_t^{\Theta} - \bar{A}_c^{\Theta} + \bar{A}_c^{\Theta} - A'^{\Theta})^{\top} (A_t^{\Theta} - \bar{A}_c^{\Theta} + \bar{A}_c^{\Theta} - A'^{\Theta}) \right] \\
&= \frac{1}{2} \sum_{t=1}^T \left[\|A_t^{\Theta} - \bar{A}_c^{\Theta}\|_2^2 + \|\bar{A}_c^{\Theta} - A'^{\Theta}\|_2^2 \right] \\
&\quad + \left(\sum_{t=1}^T (A_t^{\Theta} - \bar{A}_c^{\Theta}) \right)^{\top} (\bar{A}_c^{\Theta} - A'^{\Theta}) \\
&= \sum_{t=1}^T \frac{1}{2} \|A_t^{\Theta} - \bar{A}_c^{\Theta}\|_2^2 + \frac{T}{2} \|\bar{A}_c^{\Theta} - A'^{\Theta}\|_2^2 \\
&\quad + (T \bar{A}_c^{\Theta} - \sum_{t=1}^T A_t^{\Theta})^{\top} (\bar{A}_c^{\Theta} - A'^{\Theta}) \\
&= \sum_{t=1}^T d_{2,\Theta}(A_t, \bar{A}_c) + T d_{2,\Theta}(\bar{A}_c, A')
\end{aligned}$$

Note that in the fourth line we take the dot product with the matrices being in vectorized form and that $\bar{A}_c^{\Theta} = \frac{1}{T} \sum_{t=1}^T A_t^{\Theta}$. Note that it follows that $\bar{A}_c^{\Theta}(i, j) = \sqrt{\theta(i, j)} \bar{A}_c(i, j)$. \square

We restate the next theorem and give its proof:

Theorem 4.4. $A_c(i, j) = \Pr[i \text{ and } j \text{ in the same district}]$.

Proof. By definition of the redistricting adjacency matrices and condition (3.1) for **iid** sampling we have that:

$$\begin{aligned}
A_c(i, j) &= \mathbb{E}_{A_t \sim \mathcal{M}}[A_t(i, j)] \\
&= (1) \Pr[i \text{ and } j \text{ are in the same district}] + (0) \Pr[i \text{ and } j \text{ are not in the same district}] \\
&= \Pr[i \text{ and } j \text{ are in the same district}]
\end{aligned}$$

\square

We restate the next theorem and give its proof:

Theorem 4.5. *If we sample $T = \frac{1}{\epsilon^2} \ln \frac{n}{\delta}$ iid samples, then with probability at least $1 - \delta$, we have that $\forall i, j \in V : |\bar{A}_c(i, j) - A_c(i, j)| \leq \epsilon$.*

Proof. For a given $i, j \in V$ by the Hoeffding bound we have that:

$$\begin{aligned} \Pr[|\bar{A}_c(i, j) - A_c(i, j)| \leq \epsilon] &\geq 1 - 2e^{-2\epsilon^2 T} \\ &\geq 1 - 2e^{-2\epsilon^2 \frac{1}{\epsilon^2} \ln \frac{n}{\delta}} \geq 1 - 2(e^{2 \ln \frac{n}{\delta}})^{-1} \geq 1 - 2\frac{\delta^2}{n^2} \end{aligned}$$

Now we calculate the following event:

$$\begin{aligned} &\Pr(\{\forall i, j \in V : |\bar{A}_c(i, j) - A_c(i, j)| \leq \epsilon\}) \\ &= 1 - \Pr(\{\exists i, j \in V : |\bar{A}_c(i, j) - A_c(i, j)| > \epsilon\}) \\ &\geq 1 - \sum_{i, j \in V} 2\frac{\delta^2}{n^2} \geq 1 - 2\delta^2 \frac{(n^2 - n)}{n^2} \geq 1 - \delta^2 \geq 1 - \delta \quad (\text{since } \delta \in (0, 1)) \end{aligned}$$

□

We restate the next theorem and give its proof:

Theorem 4.6. Let $\max_{i, j \in V} \sqrt{\theta(i, j)} = \rho$, if we have $T = \frac{\rho n^2}{\epsilon} \ln \frac{n}{\delta}$ *iid* samples, then $d_{2, \Theta}(\bar{A}_c, A_c) \leq \epsilon$ with probability at least $1 - \delta$.

Proof. Applying Theorem (4.5) with ϵ set to $\frac{\sqrt{\epsilon}}{\sqrt{\rho n}}$, we get that with probability at least $1 - \delta$, $|\bar{A}_c(i, j) - A_c(i, j)| \leq \frac{\sqrt{\epsilon}}{\sqrt{\rho n^2}}$. It follows that:

$$\begin{aligned} d_{2, \Theta}(\bar{A}_c, A_c) &= \frac{1}{2} \sum_{i, j \in V} \theta(i, j) (\bar{A}_c(i, j) - A_c(i, j))^2 \\ &\leq \frac{1}{2} \sum_{i, j \in V} \theta(i, j) \left(\frac{\sqrt{\epsilon}}{\sqrt{\rho n}} \right)^2 \leq \frac{1}{2} \sum_{i, j \in V} \frac{\epsilon}{n^2} \\ &\leq \frac{1}{2} \frac{\epsilon}{n^2} \frac{n^2 - n}{2} \leq \epsilon \end{aligned}$$

□

We restate the next theorem and give its proof:

Theorem 4.7. Given the population centroid A_c , the population medoid A^* can be obtained by solving a constrained min k -cut problem.

Proof. From Theorem 4.2, the population medoid is a valid redistricting map A for which $d_{2, \Theta}(A, A_c)$ is minimized. Note that since A is a redistricting map, unlike A_c it must be a binary matrix. Therefore, $|A(i, j) - A_c(i, j)| = (1 - A_c(i, j)) + (2A_c(i, j) - 1)(1 - A(i, j))$, where this identity can be verified by plugging 0 or 1 for $A(i, j)$ and seeing that it leads to an equality. Define the matrix B as a “complement” of A . Specifically, $B(i, j) = 1 - A(i, j)$. It follows that $B(i, j) = 1$ if and only if i and j are in different partitions and $B(i, j) = 0$ otherwise. Clearly, B is a binary matrix. We can

obtain the following:

$$\begin{aligned}
d_{2,\Theta}(A, A_c) &= \frac{1}{2} \sum_{i,j \in V} \theta(i, j) (A(i, j) - A_c(i, j))^2 \\
&= \frac{1}{2} \sum_{i,j \in V} \theta(i, j) ((1 - A_c(i, j)) + (2 A_c(i, j) - 1)(1 - A(i, j)))^2 \\
&= \frac{1}{2} \sum_{i,j \in V} \theta(i, j) ((1 - A_c(i, j)) + (2 A_c(i, j) - 1)B(i, j))^2 \\
&= \frac{1}{2} \sum_{i,j \in V} \theta(i, j) ((1 - A_c(i, j))^2 + 2(1 - A_c(i, j))(2 A_c(i, j) - 1)B(i, j) + (2 A_c(i, j) - 1)^2 B^2(i, j)) \\
&= \frac{1}{2} \sum_{i,j \in V} \theta(i, j) ((1 - A_c(i, j))^2 + 2(1 - A_c(i, j))(2 A_c(i, j) - 1)B(i, j) + (2 A_c(i, j) - 1)^2 B(i, j)) \\
&= \frac{1}{2} \sum_{i,j \in V} \theta(i, j) (A_c^2(i, j) - 2 A_c(i, j) + 1) \\
&\quad + \frac{1}{2} \sum_{i,j \in V} \theta(i, j) (2 A_c(i, j) - 1)B(i, j)
\end{aligned}$$

Note that the first term in the last equality is a constant and has no dependence on B . Hence the full optimization problem is the following:

$$\min_B \sum_{i,j \in V} s(i, j) B(i, j) \tag{6}$$

$$\text{s.t. } B \text{ is a } k \text{ partition that leads to a valid redistricting map} \tag{7}$$

where the weight $s(i, j)$ is equal to $s(i, j) = \frac{1}{2}\theta(i, j)(2 A_c(i, j) - 1)$. Clearly, this is a constrained min k -cut instance where the partition has to be a valid redistricting map. \square

Here we show a negative result similar to theorem 4.8 but for redistricting maps.

Theorem A.1. *There exists a distribution over redistricting maps for which the expected map can be estimated to an arbitrary error ϵ with a polynomial number of **iid** samples. However, by only selecting a sampled point we cannot: (1) Obtain a map that is arbitrarily close to the medoid map. (2) Obtain a map whose medoid cost function value is arbitrarily close to the minimum cost function value.*

Proof. Consider the hypothetical state shown in figure 5 where vertices v_1 and v_4 are further subdividing into two vertices each. We wish to divide the state into 2 districts ($k = 2$). Since each vertex has a weight of 1, except vertices $\{a_1, b_1, a_4, b_4\}$ which each have a weight of $\frac{1}{2}$, then each district should have a population of 2 to enforce the equal population rule with a tolerance less than 0.25.

Denoting the set of all vertices by V and letting $V' = \{a_1, b_1, a_4, b_4\}$, then the weight parameters of our weighted distance measure are defined as follows:

$$\theta(i, j) = \begin{cases} \epsilon & \text{if } i \text{ \& } j \in V' \\ \frac{1}{2} & \text{if } i \in V - V', j \in V' \text{ or } i \in V', j \in V - V' \\ 1 & \text{otherwise} \end{cases}$$

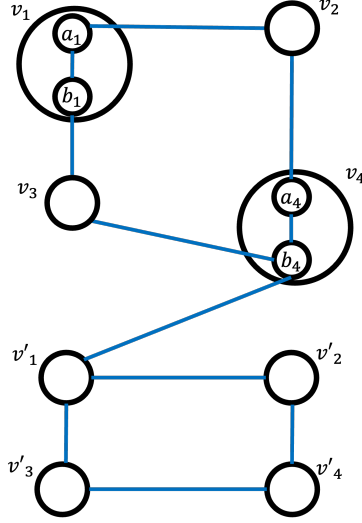


Figure 5: The graph shows a hypothetical state. Blue edges indicate that the vertices are adjacent geographically. All vertices have a weight (population of 1), except for states $\{a_1, b_1, a_4, b_4\}$ which have a weight of $\frac{1}{2}$.

Where $0 < \epsilon \leq 1$. Now, consider the maps M_1, M_2, M_3 , and M_4 shown in figure 6. Based on the definition of the weighted distance measure, it is not difficult to see that given maps M_s and M_t , then $d_\Theta(M_s, M_t)$ can be computed visually by drawing the adjacent graphs of M_s and M_t and then finding the minimum number of edges that have to be deleted and added to M_s to produce M_t and adding the weighted $\theta(i, j)$ of these edges. By following this procedure, we can show that $d_\Theta(M_1, M_3) = 6 + 4\epsilon$ for example as shown in figure 7. Here we list all distances:

$$\begin{aligned}
 d_\Theta(M_1, M_2) &= 4 \\
 d_\Theta(M_1, M_4) &= d_\Theta(M_2, M_4) = 2 + 4\epsilon \\
 d_\Theta(M_1, M_3) &= d_\Theta(M_2, M_4) = (2 + 4\epsilon) + 4 = 6 + 4\epsilon \\
 d_\Theta(M_3, M_4) &= 4
 \end{aligned}$$

Given a map M , the medoid cost function is defined as $f(M) = \sum_{M' \in \mathcal{M}} p_{M'} d(M, M')$. Let the probabilities for the redistricting maps be assigned as follows: $p_1 = p_2 = p_3 = \frac{1-\delta}{3}$ whereas $\Pr[\text{Sampling a Map } M \notin \{M_1, M_2, M_3\}] = \delta > 0$. Accordingly, $p_5 \leq \delta$. Further, since $\theta(i, j) \leq 1, \forall i, j \in V$, then we can upper bound the maximum distance between any redistricting maps D by considering the highest number of edges that can be deleted and added from one map to produce another, therefore $D \leq 2 \binom{|V|}{2} = |V|(|V| - 1) = 10 \times 9 = 90$ since $|V| = 10$ (see, figure 5). The medoid cost function can be lower bounded for M_1, M_2 , and M_3 and upper bounded for M_4 as

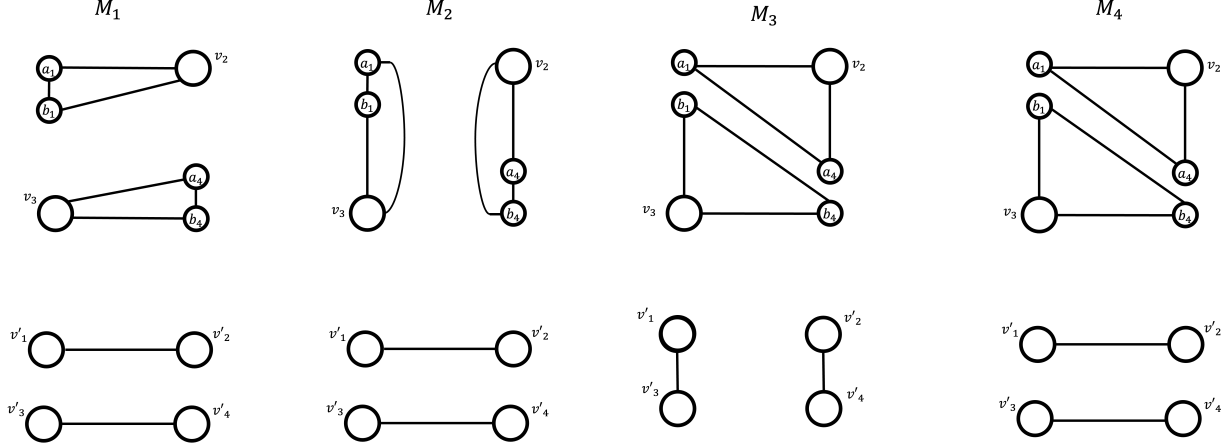


Figure 6: Maps M_1, M_2, M_3 , and M_4 . Vertices in the same district are connected with edges.

shown below:

$$\begin{aligned}
f(M_1) &> \frac{1-\delta}{3}[d(M_1, M_2) + d(M_1, M_3)] = \frac{1-\delta}{3}(10 + 4\epsilon) \\
f(M_2) &> \frac{1-\delta}{3}[d(M_1, M_2) + d(M_2, M_3)] = \frac{1-\delta}{3}(10 + 4\epsilon) \\
f(M_3) &> \frac{1-\delta}{3}[d(M_1, M_3) + d(M_2, M_3)] = \frac{1-\delta}{3}(12 + 8\epsilon) \\
f(M_4) &< \frac{1-\delta}{3}[d(M_1, M_4) + d(M_2, M_4) + d(M_3, M_4)] + \delta D = \frac{1-\delta}{3}(8 + 8\epsilon) + 90\delta
\end{aligned}$$

If $\delta < \frac{1}{271}$, then $90\delta < \frac{1-\delta}{3}$ and therefore $f(M_4) \leq \frac{1-\delta}{3}(9 + 8\epsilon)$. Set $\epsilon = \frac{1}{1000}$ and $\delta \leq \frac{1}{1000} < \frac{1}{271}$ and with $1 - (p_1 + p_2 + p_3) = \delta$, then $\frac{1-\delta}{3}(1 - 4\epsilon) > 0.331$ and $\frac{(10+4\epsilon)}{(9+8\epsilon)} > 1.11$. With the true medoid denoted by M^* , then we have: $\min_{i \in \{1,2,3\}} \frac{f(M_i)}{f(M^*)} \geq \min_{i \in \{1,2,3\}} \frac{f(M_i)}{f(M_4)} \geq \frac{\frac{1-\delta}{3}(10+4\epsilon)}{\frac{1-\delta}{3}(9+8\epsilon)} > 1.11$ and therefore the medoid cannot be M_1, M_2 , or M_3 . Further, it follows by the triangle inequality that $\forall i \in \{1, 2, 3\} : f(M_i) \leq f(M^*) + d(M_i, M^*)$, thus $d(M_i, M^*) \geq \frac{1-\delta}{3}(1 - 4\epsilon)$, since otherwise $f(M^*) + d(M_i, M^*) \leq f(M_4) + d(M_i, M^*) \leq \frac{1-\delta}{3}(9 + 8\epsilon) + \frac{1-\delta}{3}(1 - 4\epsilon) \leq \frac{1-\delta}{3}(10 + 4\epsilon)$. Therefore, we cannot get a map which gives an arbitrarily small approximation error of the medoid or whose approximation error of the medoid cost function is arbitrarily small by pure sampling. More specifically, since $\forall i \in \{1, 2, 3\} : d(M_i, M^*) \geq \frac{1-\delta}{3}(1 - 4\epsilon) > 0.331$, then we have the following:

$$\begin{aligned}
&\Pr[\text{Obtaining a map } M \text{ such that } d(M, M^*) < 0.331 \text{ in a given } T \text{ iid samples}] \\
&= 1 - \Pr[\text{Not Obtaining a map } M \text{ such that } d(M, M^*) < 0.331 \text{ in a given } T \text{ iid samples}] \\
&\leq 1 - \Pr[\text{Obtaining a map } M \in \{M_1, M_2, M_3\} \text{ in a given } T \text{ iid samples}] \\
&= 1 - (1 - \delta)^T
\end{aligned}$$

if we choose an arbitrarily small number ρ , then we just need to set $\delta = 1 - \sqrt[T]{1 - \rho}$ to make the probability of obtaining a map M with $d(M, M^*) < 0.331$ in T iid samples arbitrarily be upper bounded by ρ . This proves (1), i.e. the medoid cannot be approximated to an arbitrarily small error by only selecting a sampled map.

By following a similar procedure, we can show that with arbitrarily small probability we would obtain a map M for which $\frac{f(M)}{f(M^*)} \leq \frac{10+4\frac{1}{100}}{9+8\frac{1}{100}} > 1.11$ given T iid samples. This proves (2), i.e. the medoid cost function cannot be approximated to an arbitrarily small error by only selecting a sampled map.

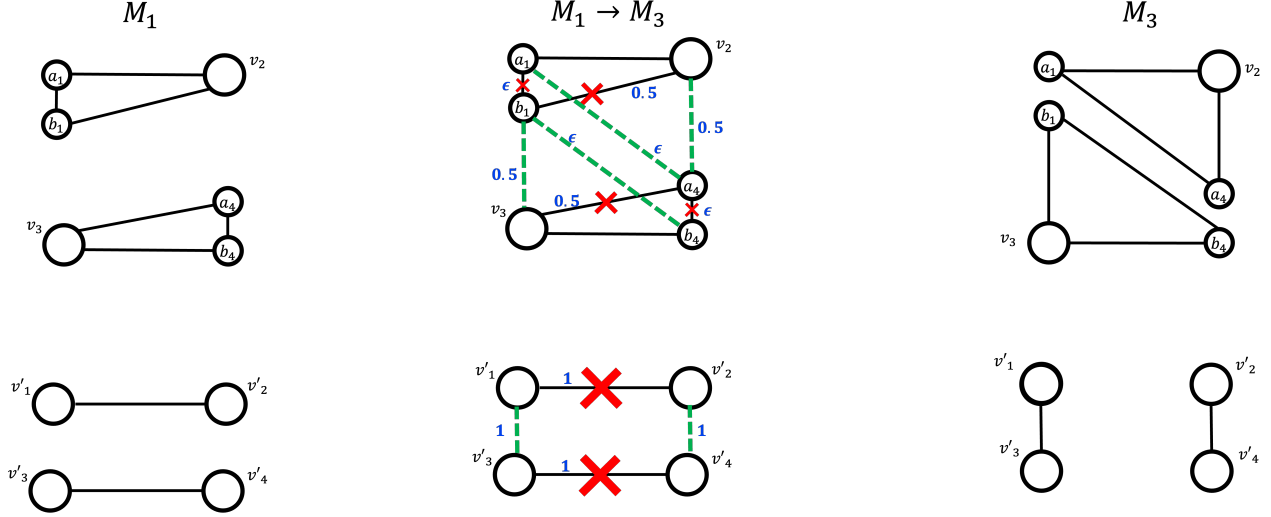


Figure 7: The first map is M_1 and the last is M_3 . The middle map shows the edges the should be deleted from M_1 (marked with **X**) and the edges should be added to M_1 (dashed green edges) to produce M_3 . The weight of each edge that is deleted or added is shown next to it in blue. By adding the weights we get that $d_{\Theta}(M_1, M_3) = 6 + 4\epsilon$.

Convergence to the centroid is easy, by a straightforward application of the generalized Hoeffding inequality (see [Ashtiani et al., 2016] for example). \square

B Additional Experimental Results

B.1 Convergence to the centroid

As a reminder to further test the robustness of our results and see the convergence, all calculations are done 3 times each time starting from a specific seed map. For example, we estimate the centroid three times, by sampling starting from seed maps s_1 , s_2 , and s_3 ⁷ and as a result we end up with three centroids c_1 , c_2 , and c_3 . Here we further verify the convergence of the centroids by showing that the final estimated centroids are close to each other. In fact, if we denote the smallest $d_{2,\Theta}(\cdot, \cdot)$ distance between a sampled map and any of the centroids c_1 , c_2 , or c_3 by $d_{2,\Theta_{\min}}$. Then we consistently find –for all states (NC,MD,PA) and all distance measures (unweighted and population-weighted)– that for any two estimated centroids c_i and c_j that $d_{2,\Theta}(c_i, c_j) \leq d_{2,\Theta_{\min}}$ by at least 3 orders of magnitude. This is strong evidence that while the differences in the estimation may be large in value, they are very small relative to the distances between other maps. Therefore, at this scale the estimation error is small. Table 1 shows the maximum $d_{2,\Theta}(\cdot, \cdot)$ distance between any two estimated centroid and $d_{2,\Theta_{\min}}$.

⁷One of the seed maps is an already enacted map whereas the other two are produced using optimization functions from the GerryChain toolbox: <https://github.com/mggg/GerryChain>.

Table 1: Maximum Distance Between Any Two Centroids vs Minimum Distance between a Centroid and a Sampled Map

STATE	Distance Measure	$\max_{i,j \in \{1,2,3\}} d_{2,\theta}(c_i, c_j)$	$d_{2,\theta \min}$
NC	Unweighted	8.6297×10^1	1.059368×10^5
NC	Population-Weighted	1.1248×10^9	1.371594×10^{12}
MD	Unweighted	4.0852×10^1	7.243768×10^4
MD	Population-Weighted	4.1914×10^8	7.315014×10^{11}
PA	Unweighted	2.2782×10^3	1.099201×10^6
PA	Population-Weighted	4.5747×10^9	2.052592×10^{12}

B.2 Distance Histograms and Detecting Gerrymandered Maps

Here we produce the histogram maps for all states and all distance measures. We produce 3 histograms for each state and distance measure each starting from a specific centroid and by sampling from its corresponding seed, e.g. we sample maps starting from seed s_1 and calculate $d_{2,\theta}(M, c_1)$ between a sampled map M and centroid c_1 to construct one histogram. We find similar observations to figure 2, indeed we see that the shape of the histograms is stable across all states, distances, and centroids. I.e., all of the distance histograms peak in the middle and fall away from the middle similar to a normal distribution. Further, our observations about the gerrymandered maps of NC (figure 8) and PA (figure 9) still hold. Specifically, gerrymandered maps are outliers with large distances and appear at the right tail of the distribution whereas the remedial maps have much smaller distances and appear around the peak of the histogram.

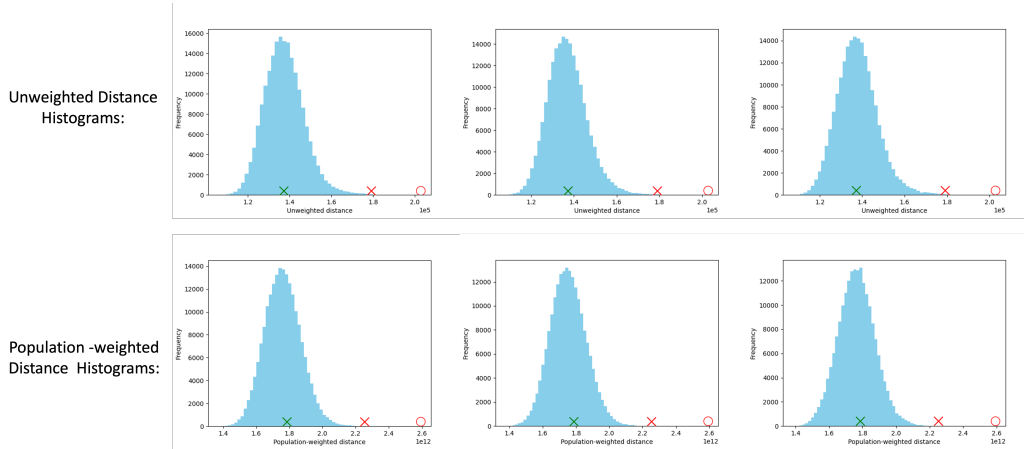


Figure 8: Distance histograms for NC, the distances of gerrymandered maps are indicated with red markers whereas the distances of the remedial maps are indicated with green markers. The \circ and the \times are for 2011 and 2016 enacted maps, respectively.

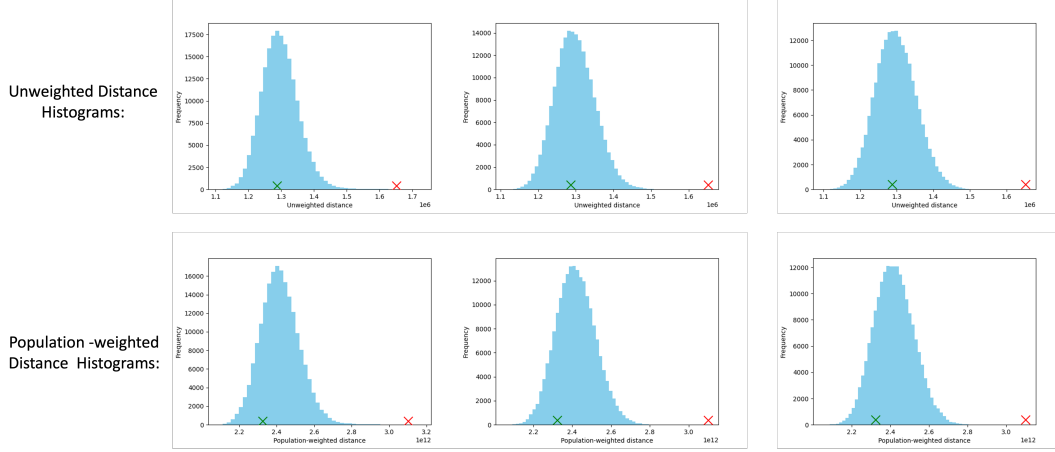


Figure 9: Distance histograms for PA, the distances of gerrymandered maps are indicated with red markers whereas the distances of the remedial maps are indicated with green markers..

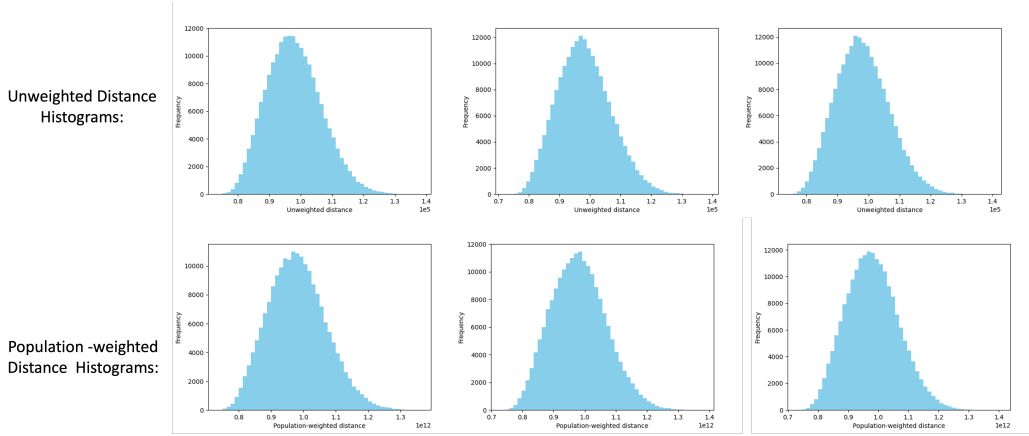


Figure 10: Distance histograms for MD.

B.3 Finding the Medoid

Similar to the previous experiments, we produce three medoids, one for each state and distance measure. Having chosen the state and distance seed (unweighted or population-weighted), then for a given centroid c_i and its corresponding seed s_i , we start by sampling 200,000 maps from the seed and pick the sampled map M whose distance $d_{2,\theta}(M, c_i)$ is the smallest. We refer to this map as the *initial medoid*. Clearly, we would have 3 such maps for each state and distance measure. Having found the initial map, we start sampling again but this time starting from the initial map. However, we modify the transition in the **ReCom** chain. Specifically, if we are at a state (map) M , then we only transition to a new state (map) M' if its closer to the centroid, i.e. $d_{2,\theta}(M', c_i) < d_{2,\theta}(M, c_i)$. Doing this for 200,000 iterations, we obtain the *final medoid*. Again we would have 3 final medoid maps for each state and distance measure.

Relative Error Measure: We have seen in the previous section that we have convergence in the centroid and therefore we assume that we are dealing with one centroid \bar{A}_c and that \bar{A}_c is a very good approximation of the population centroid A_c . Suppose the candidate medoid map we have is

\hat{M}_1 , then the measure of how good the map \hat{M}_1 is as a medoid is the medoid cost function which equals:

$$f(\hat{M}_1) = \mathbb{E}_{M' \sim \mathcal{D}(\mathcal{M})} [d(\hat{M}_1, M')] = \sum_{M' \in \mathcal{M}} p_{M'} d(\hat{M}_1, M')$$

Given T samples we can approximate the medoid cost function by:

$$\hat{f}(\hat{M}_1) = \frac{1}{T} \sum_{t=1}^T d_{\Theta}(\hat{M}_1, M_t)$$

Further, using the decomposition theorem (4.2), we have the following:

$$\hat{f}(\hat{M}_1) = \frac{1}{T} \sum_{t=1}^T d_{\Theta}(\hat{M}_1, M_t) = d_{2,\Theta}(\hat{M}_1, \bar{A}_c) + \frac{1}{T} \sum_{t=1}^T d_{2,\Theta}(A_t, \bar{A}_c)$$

Since the second term does not depend on \hat{M}_1 , it follows that the distance to the centroid $d_{2,\Theta}(\hat{M}_1, \bar{A}_c)$ decides the medoid cost function $\hat{f}(\hat{M}_1)$. Further, given two candidate medoids: \hat{M}_1 and \hat{M}_2 , we note that the absolute difference in \hat{f} between the two maps is simply:

$$|\hat{f}(\hat{M}_1) - \hat{f}(\hat{M}_2)| = |d_{2,\Theta}(\hat{M}_1, \bar{A}_c) - d_{2,\Theta}(\hat{M}_2, \bar{A}_c)| \quad (8)$$

Where again we used the decomposition theorem (4.2), i.e. the terms involving the centroid cancel out. Clearly, one map would be closer than the other to the centroid, i.e. $d_{2,\Theta}(\hat{M}_1, \bar{A}_c) \leq d_{2,\Theta}(\hat{M}_2, \bar{A}_c)$ or $d_{2,\Theta}(\hat{M}_2, \bar{A}_c) \leq d_{2,\Theta}(\hat{M}_1, \bar{A}_c)$. We are interested in knowing how well the worse performing map approximates the medoid cost function relative to the better map. We can use the relative performance measure, which can be calculated using only $d_{2,\Theta}(\hat{M}_2, \bar{A}_c)$ and $d_{2,\Theta}(\hat{M}_1, \bar{A}_c)$:

$$\mathbf{RE}(M_1, M_2) = \frac{|d_{2,\Theta}(\hat{M}_1, \bar{A}_c) - d_{2,\Theta}(\hat{M}_2, \bar{A}_c)|}{\min\{d_{2,\Theta}(\hat{M}_1, \bar{A}_c), d_{2,\Theta}(\hat{M}_2, \bar{A}_c)\}}$$

We use the relative error measure $\mathbf{RE}(\cdot, \cdot)$ to see how the final medoids approximate the medoid cost function relative to one another.

General Observations and Conclusion: Here we note the observations we reach from the following subsections: (1) For a given state and seed, the initial medoids are the same regardless of distance used (unweighted or population-weighted). (2) For NC and MD, the final medoids are visually very similar, however for PA which is much larger we notice significant differences. (3) Medoid maps can lead to different election results even if they are visually very similar and very close in terms of distance d_{Θ} . In fact, maps can lead to different election results even if when the distance between them is smaller than the distance between one of them and any other sampled map. This can be explained based on small districts which include few vertices but have high relative population in their vertices. (4) Medoid maps do not lead to rare election outcomes and mostly the election outcome is at the peak of the election histogram or close to it. (5) The relative error measure $\mathbf{RE}(\cdot, \cdot)$ over final medoid is in general very small, at most equal to 3.23%. Further, if one was to use the initial map instead the relative can be much larger going from around 0.7% to around 15.0%. It is possible that we can explain the fact that we find final medoids with small relative error but that are still different by the fact that the medoid may not be unique. Regardless, we believe the final medoids maps we obtain are useful as starting maps that can be refined to draw final redistricting maps to be enacted.

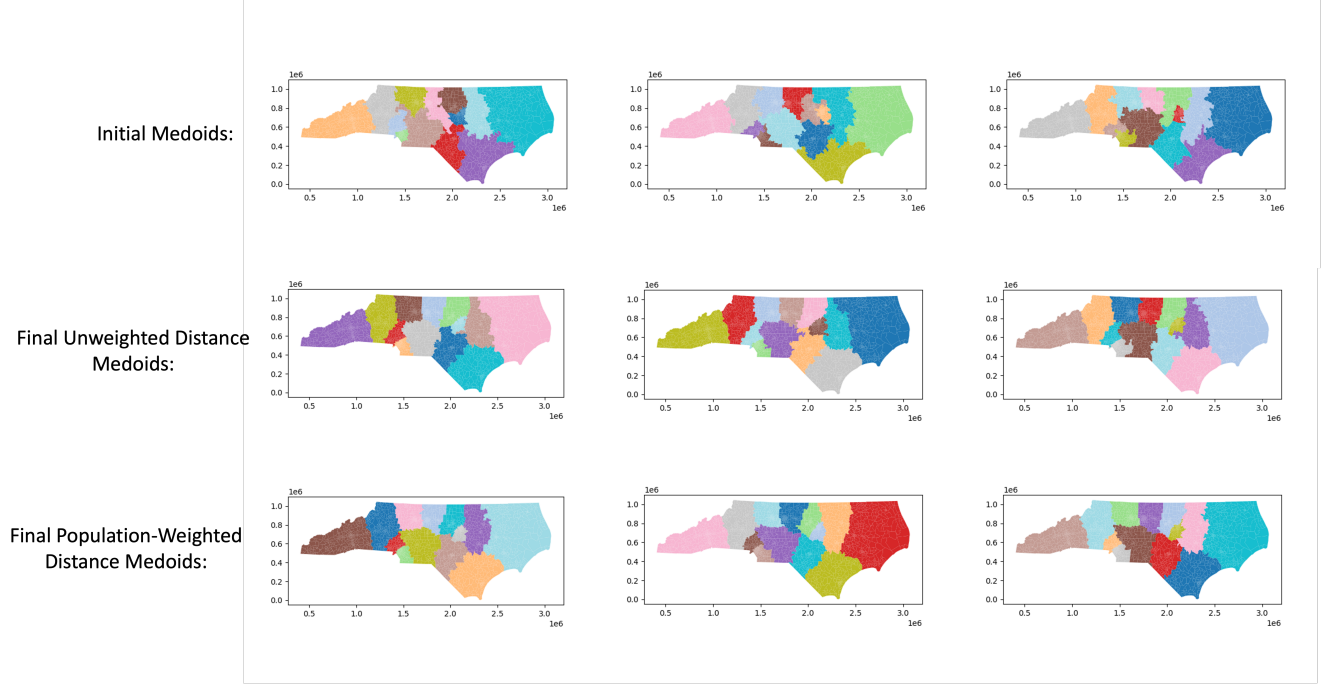


Figure 11: NC Medoids. (Top Row): Initial Medoids, (Middle Row): Final Unweighted Distance Medoids, and (Bottom Row): Final Population-Weighted Distance Medoids. Each column is for a specific seed and its associated centroid.

B.3.1 Initial Medoids and Final Medoids

Figures (11), (12), and (13) show the initial and final medoids for NC, MD, and PA, respectively. We note that in all figures, that maps in the first column are all using seed s_1 and centroid c_1 , the second column using seed s_2 and centroid c_2 , and the third column using seed s_3 and centroid c_3 . Further, the initial medoid maps are found to be the same for both distances (unweighted or population-weighted). In general, we notice that the NC and MD final medoid maps are much similar to one another than PA as there are large regions in PA that are clearly assigned to different districts.

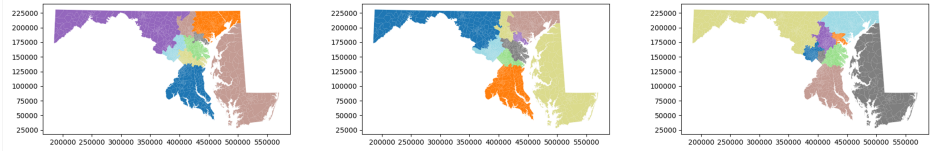
B.3.2 Relative Error $RE(.,.)$ between the Final Medoids

Since we have three final medoids for each state and distance measure, we report the maximum relative error value that can be obtained using any pair of maps. Table 2 shows the maximum relative error percentage value, clearly the largest relative error value is at most around 3.23%. To further note the importance of our heuristic, if we only an initial map instead the relative error can be much larger in comparison to the best final medoid map. For example, in the case of MD for the unweighted distance it can be as large as 11% whereas it is around 3.23%, in the case of PA for the weighted distance it can be as large as 14.97% whereas it is around 0.67%.

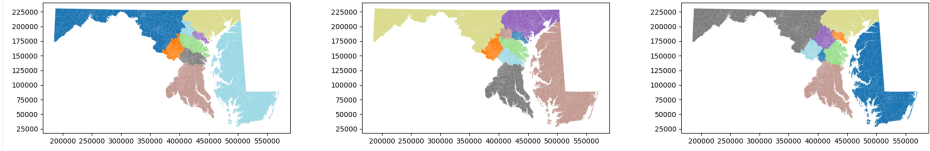
B.3.3 Election Histograms and Medoid Election Results

We show the election histogram for each state using votes for a specific election such as the senate election of 2016 (see the title above each histogram for the votes used). According to the distribution

Initial Medoids:



Final Unweighted Distance Medoids:



Final Population-Weighted Distance Medoids:

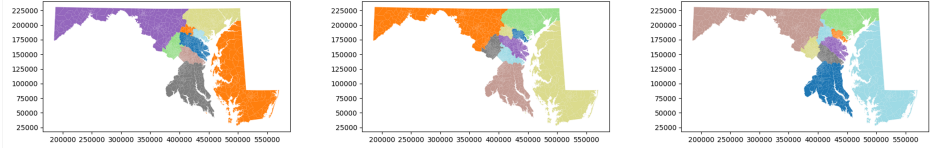
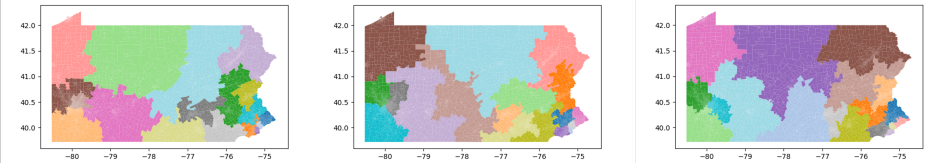
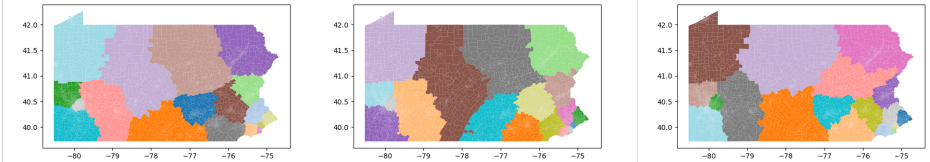


Figure 12: MD Medoids. (Top Row): Initial Medoids, (Middle Row): Final Unweighted Distance Medoids, and (Bottom Row): Final Population-Weighted Distance Medoids. Each column is for a specific seed and its associated centroid.

Initial Medoids:



Final Unweighted Distance Medoids:



Final Population-Weighted Distance Medoids:

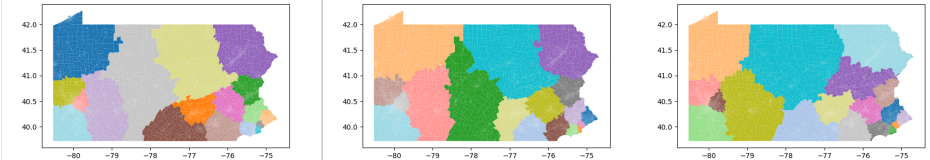


Figure 13: PA Medoids. (Top Row): Initial Medoids, (Middle Row): Final Unweighted Distance Medoids, and (Bottom Row): Final Population-Weighted Distance Medoids. Each column is for a specific seed and its associated centroid.

Table 2: Maximum Relative Error **RE** between final medoids for each state and distance measure

STATE	Distance Measure	Max RE(.,) Percentage Value Over Final Medoid Pair
NC	Unweighted	0.89279
NC	Population-Weighted	1.098535
MD	Unweighted	3.22557
MD	Population-Weighted	1.42005
PA	Unweighted	2.01045
PA	Population-Weighted	0.66659

of votes in each district the number of seats won by a specific party can be calculated. Since we have two-party results, we show only the seats for one party (Democratic party). Finding election histograms using sampling methods is well-established [DeFord et al., 2019, Herschlag et al., 2020] therefore we show only one histogram for each state. We note that the election histograms are the same independent of the choice of seed (as expected). Further, election histograms are not related to a centroid or a chosen distance measure. For each state and distance measure, we show mark the number of seats for the final medoid maps. In general, medoid maps lead to election results that have high probability, often the outcome with the highest or second highest probability. The medoid which leads to the least likely outcome is weighted medoid 2 for NC, which results in an outcome that occurs only 5% of the times for the presidential 2016 votes. However, this is not similar to what is found in gerrymandered maps as they lead to much lower probability [Mattingly and Vaughn, 2014]. Moreover, we find that the election outcomes of different medoids can overlap. In fact, in the case of NC, the unweighted medoids all lead to the same election outcomes. In the case of MD, the population-weighted medoids also all lead to the same election outcomes. Interestingly, for MD the unweighted medoids 1 and 2 (call them M_1 and M_2 , respectively) lead to different election outcomes for the Attorney General 2018 election despite the fact that they are visually very similar. In fact, not only are M_1 and M_2 very similar, but by when sampling 50,000 maps and calculating their distance from M_1 we find that smallest unweighted distance we can find is 5.96×10^4 whereas the unweighted distance between M_1 and M_2 is 3.92×10^4 which is around $0.65 \times 5.96 \times 10^4$ and therefore M_2 is significantly closer to M_1 than any other map, yet M_1 and M_2 can still lead to different election outcomes.

See figures 14, 15, 16, 17, 18, and 19 for the election histograms and the medoid election outcomes.

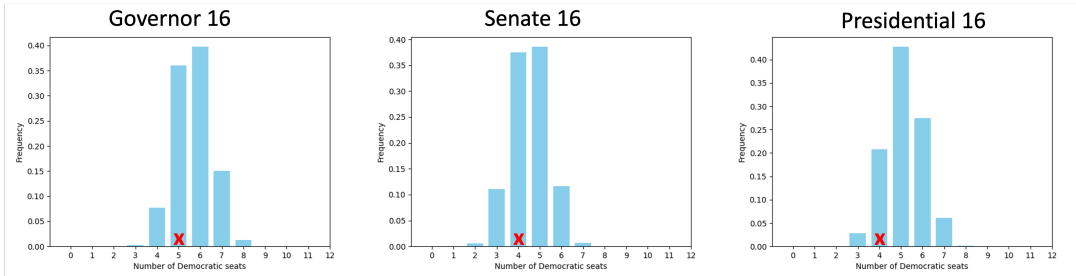


Figure 14: NC Election Histograms and unweighted final medoid outcomes. All unweighted medoids in this case lead to the same outcome and it is marked with **X**.

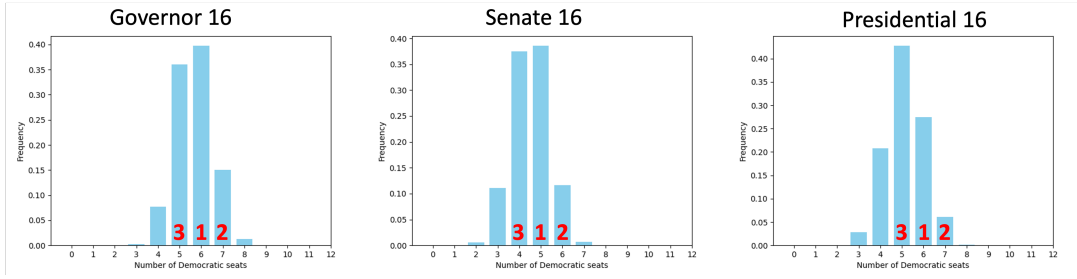


Figure 15: NC election histograms and population-weighted final medoid outcomes. The outcome of each medoid is marked with the medoid's index, i.e. 1,2, or 3.

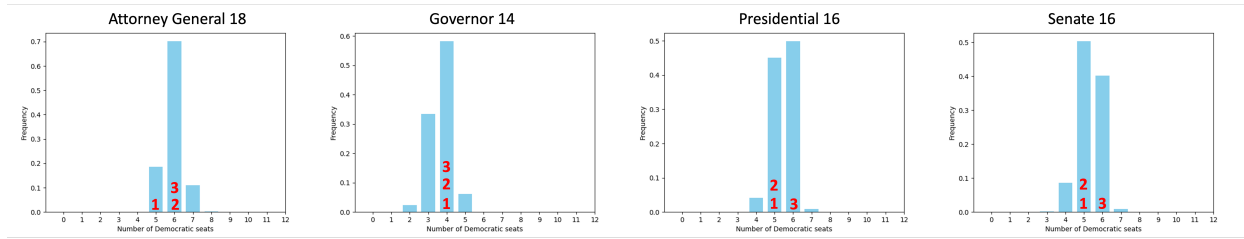


Figure 16: MD election histograms and unweighted final medoid outcomes. The outcome of each medoid is marked with the medoid's index, i.e. 1,2, or 3.

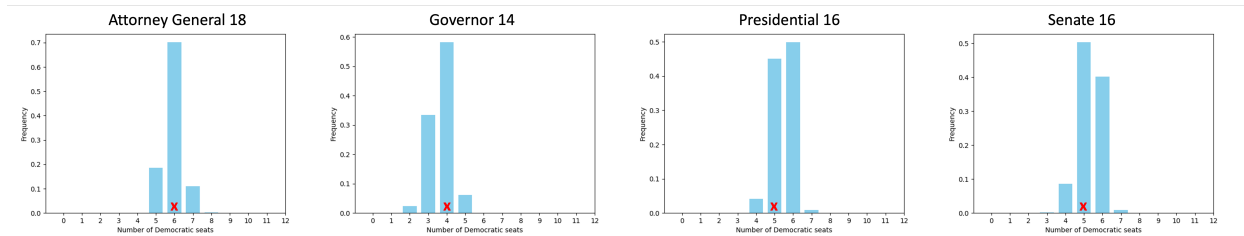


Figure 17: MD election histograms and population-weighted final medoid outcomes. All weighted medoids in this case lead to the same outcome and it is marked with X.

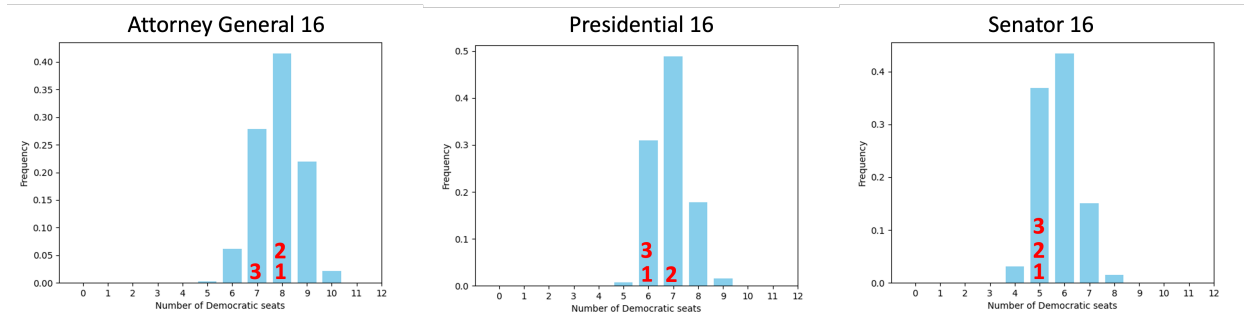


Figure 18: PA election histograms and unweighted final medoid outcomes. The outcome of each medoid is marked with the medoid's index, i.e. 1,2, or 3.

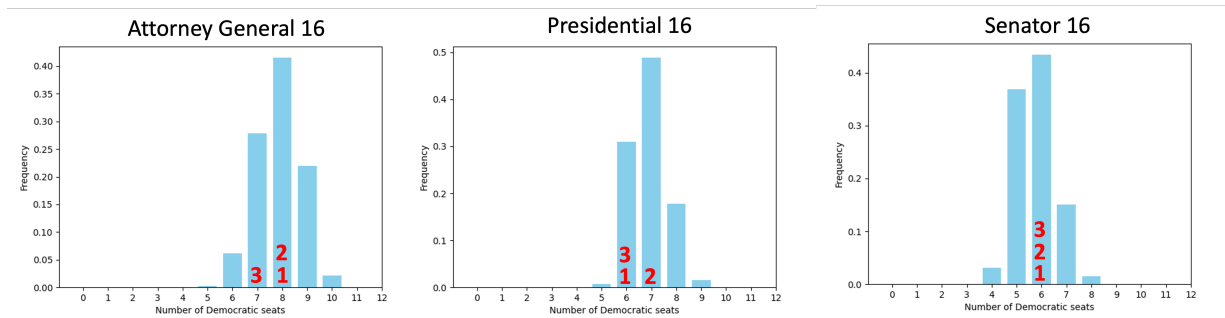


Figure 19: PA election histograms and population-weighted final medoid outcomes. The outcome of each medoid is marked with the medoid's index, i.e. 1, 2, or 3.